NPS72-86-003CR

NAVAL POSTGRADUATE SCHOOL
Monterey, California

ANALYTICAL AND NUMERICAL COMPUTATION OF

RING-SYMMETRIC SPACECRAFT EXHAUST PLUMES

by

Joseph Falcovitz

December 1986

NAVAL POSTGRADUATE SCHOOL
Monterey, California

RADM R. C. Austin
Superintendent

D. A. Schrady
Provost

The work reported herein was performed for the Naval Postgraduate School by
Dr. Joseph Falcovitz under contract N62271-86-M-0214. The work presented in
this report is in support of "Rarefied Gas Dynamics of Laser Exhaust Plume"
sponsored by the Strategic Defense Initiative Office/Directed Energy Office.
This is a partial report for that contract. The work provides information
concerning continuum approximation of flow at the fringes of spacecraft
exhaust plumes; it is to be used in conjunction with an ambient scattering
model. The project at the Naval Postgraduate School is under the cognizance
of Distinguished Professor A. E. Fuhs who is principal investigator.

Reproduction of all or part of this report is authorized.

Prepared by:

REPORT DOCUMENTATION PAGE

1a REPORT SECURITY CLASSIFICATION	1b RESTRICTIVE MARKINGS
UNCLASSIFIED	NONE
2a SECURITY CLASSIFICATION AUTHORITY	3. DISTRIBUTION/AVAILABILITY OF REPORT
2b DECLASSIFICATION/DOWNGRADING SCHEDULE	Approved for Public Release; Distribution Unlimited

4 PERFORMING ORGANIZATION REPORT NUMBER(S)	5. MONITORING ORGANIZATION REPORT NUMBER(S)
NPS72-86-003CR	NPS72-86-003CR

6a NAME OF PERFORMING ORGANIZATION	6b OFFICE SYMBOL (If applicable)	7a. NAME OF MONITORING ORGANIZATION
JOSEPH FALCOVITZ	72	NAVAL POSTGRADUATE SCHOOL, CODE 72

6c ADDRESS (City, State, and ZIP Code)	7b. ADDRESS (City, State, and ZIP Code)
Research Contractor Naval Postgraduate School Monterey, CA 93943-5100	Space Systems Academic Group Monterey, CA 93943-5100

8a NAME OF FUNDING/SPONSORING ORGANIZATION Strategic Defense Initiative Office	8b. OFFICE SYMBOL (If applicable) SDIO/DEO	9. PROCUREMENT INSTRUMENT IDENTIFICATION NUMBER MIPR DGAA60045

8c ADDRESS (City, State, and ZIP Code)	10. SOURCE OF FUNDING NUMBERS			
	PROGRAM ELEMENT NO.	PROJECT NO.	TASK NO	WORK UNIT ACCESSION NO.
SDIO/DEO Washington, DC 20301-7100	PE63221			

11. TITLE (Include Security Classification)

Analytic and Numerical Computation of Ring-Symmetric Spacecraft Exhaust Plumes

12 PERSONAL AUTHOR(S)
JOSEPH FALCOVITZ

13a TYPE OF REPORT	13b. TIME COVERED	14 DATE OF REPORT (Year, Month, Day)	15 PAGE COUNT
Contractor Report	FROM Aug 86 TO Dec 86	December 1986	58

16 SUPPLEMENTARY NOTATION

17 COSATI CODES			18. SUBJECT TERMS (Continue on reverse if necessary and identify by block number)
FIELD	GROUP	SUB-GROUP	Exhaust Plume, Ring Plume, Analytic Approximation, Laser Exhaust, Centered Rarefaction Waves

19 ABSTRACT (Continue on reverse if necessary and identify by block number)

A doubleheader approach to the computation of a ring-symmetric spacecraft exhaust plume is presented. We plan to use the present analytic approximation in conjunction with a model for backflow from the exhaust plume of an orbiting spacecraft, induced by oncoming ambient molecules. This process takes place in the regions of centered rarefaction waves (CRW) that flank the central plume. A semi-inverse marching characteristic scheme (SIMA) is formulated specifically for accurate computation of a CRW in two-dimensional axisymmetric coordinates, as a variant of the classical inverse marching method. It replicates a Prandtl-Meyer flow exactly, resulting in an accurate marching scheme for axisymmetric CRW. The analytic approximation to a ring-symmetric CRW is formulated in two phases. An analysis of the flow near the corner using characteristic coordinates, results in fan-wise gradients of flow variables (Riemann invariants). These gradients are then used to extrapolate the flow field along fan characteristics from the presumably Prandtl-Meyer flow at the corner, while matching exactly the cylindrically diverging flow along the unreflected portion of the CRW leading characteristic. The resulting approximation compares favorably with numerical (SIMA) computations, even at about 10 corner radii away from the corner. Closed-form expressions are obtained for lateral plume opacity at the CRW fringes.

20 DISTRIBUTION/AVAILABILITY OF ABSTRACT	21 ABSTRACT SECURITY CLASSIFICATION
☒ UNCLASSIFIED/UNLIMITED ☐ SAME AS RPT ☐ DTIC USERS	UNCLASSIFIED
22a NAME OF RESPONSIBLE INDIVIDUAL ALLEN E. FUHS, Distinguished Professor	22b TELEPHONE (Include Area Code) (408)646-2948	22c. OFFICE SYMBOL 72

i

ABSTRACT

A doubleheader approach to the computation of a ring-symmetric spacecraft exhaust plume is presented. We plan to use the present analytic approximation in conjunction with a model for backflow from the exhaust plume of an orbiting spacecraft, induced by oncoming ambient molecules. This process takes place in the regions of centered rarefaction waves (CRW) that flank the central plume. A semi-inverse marching characteristic scheme (SIMA) is formulated specifically for accurate computation of a CRW in two-dimensional axisymmetric coordinates, as a variant of the classical inverse marching method. It replicates a Prandtl-Meyer flow exactly, resulting in an accurate marching scheme for axisymmetric CRW. The analytic approximation to a ring-symmetric CRW is formulated in two phases. An analysis of the flow near the corner using characteristic coordinates, results in fan-wise gradients of flow variables (Riemann invariants). These gradients are then used to extrapolate the flow field along fan characteristics from the presumably Prandtl-Meyer flow at the corner, while matching exactly the cylindrically diverging flow along the unreflected portion of the CRW leading characteristic. The resulting approximation compares favorably with numerical (SIMA) computations, even at about 10 corner radii away from the corner. Closed-form expressions are obtained for lateral plume opacity at the CRW fringes.

ACKNOWLEDGEMENTS

TABLE OF CONTENTS

LIST OF FIGURES

LIST OF TABLES

v

NOMENCLATURE

A_0 spacecraft radius   (m)

B   breakdown parameter [2,10]

$C^{\pm}$ characteristic lines inclined at $(\theta \pm \mu)$

D   molecular diameter (hard spheres)   (m)

f   streamtube area ratio

H   special function obtained by integration across Prandtl-Meyer fan

M   Mach number

n   number density   (molecules/m^3)

p   pressure   (Pa)

S   coordinate along streamlines   (m)

T   temperature   (K)

u   flow velocity   (m/sec)

x   axial cartesian coordinate

y   radial cartesian coordinate

α fan-wise characteristic coordinate   (m)

β fan-transverse characteristic coordinate

γ ratio of specific heats

δ power for area ratio radial power-law

ε coefficient for flow angle (θ) radial logarithmic law

η length coordinate along fan characteristics (C^+) (m)

θ inclination of flow velocity vector

κ power for $\cos\theta$ radial power-law

λ coefficient for characteristic angle (ψ) radial logarithmic law

μ Mach angle $(\sin\mu = 1/M)$

ν Prandtl-Meyer function

ξ length coordinate along transverse (C^-) characteristic

σ collision cross-section πD^2 (m^2)

τ molecular opacity (expected number of collisions by a fast invading molecule)

φ collision frequency (sec^{-1})

χ inclination of C^- characteristic : $\theta - \mu$

ψ inclination of C^+ characteristic : $\theta + \mu$

ω symmetry index (0 - planar flow, 1 - axisymmetric flow)

Γ the fraction $(\gamma + 1)/(\gamma - 1)$

$(\ )_0$ a specific point in the CRW (x_0, y_0)

$(\ )_1$ nozzle exit conditions

$(\ )_L$ limiting CRW characteristic $(p = 0)$

$(\ )_f$ final CRW characteristic (boundary of numerical integration)

$(\ )_c$ corner of CRW

EMPTY PAGE

1. INTRODUCTION

The exhaust of a large space-based HF/DF chemical laser can be idealized as a zero-thrust supersonic ring-symmetric jet (Figure 1-1). Assuming a vacuum background, the exhaust plume is always flanked by a pair of ring-symmetric rarefaction waves centered at the nozzle lips (Figure 1-1). When ambient molecules traveling at orbital speed impinge obliquely at the centered rarefaction wave (CRW), they give rise to a molecular backflow of scattered exhaust species. This effect constitutes a potentially significant contribution to spacecraft contamination [1].

Most ambient molecules are stopped within several mean free paths from their point of entry into the plume. A quantitative estimate of ambient back-scattering would thus depend on the flow field at the outer (hypersonic) fringes of the lip-centered CRW. Even though the flow in those regions is generally past the point of continuum breakdown [2], the density there is reasonably well approximated by the continuum flow field, as demonstrated by Bird's Monte-Carlo simulation of a Prandtl-Meyer expansion to vacuum [3]. The evaluation of ambient scattering thus calls for an ancillary computational procedure capable of rendering the continuum flow field at a large number of points in the ring-symmetric CRW of an HF/DF laser exhaust plume.

The purpose of this report is to present a doubleheader approach to this CFD task, consisting of a specially formulated finite difference scheme valid throughout the plume and an analytic approximation for the CRW portion of the flow. This approach is motivated by the need to approximate the CRW flow field in a simple and computationally affordable way. A finite difference integration by marching out from the nozzle exit to every point in the CRW where ambient scattering is to be evaluated, is not affordable due to the very large number of such points. An interpolation from a 2-D grid of pre-computed points is affordable but rather cumbersome and complex (if only for the need to maintain an elaborate 2-D finite difference code that would make its output available to the ambient scattering code). We propose to obviate both the finite difference computation and subsequent interpolations by constructing an analytic approximation to a ring-symmetric CRW. The finite difference code "JET" that was written for the purpose of computing a ring-symmetric supersonic flow field, is thereby relegated to the role of aiding in the verification of the analytic approximation. We also use this code to obtain whole-plume solutions for the purpose of illustrating some features of the flow field by means of graphic output.

The finite difference scheme used for computing the exhaust flow field, is a modification of the well-known inverse marching characteristic method [4]. Rather than using the two velocity

components often recommended in the literature [4], we use the two Riemann invariants $(v \pm \theta)$ as flow variables. The key element in the scheme is a Semi-Inverse Marching Algorithm (SIMA). The flow is assumed to exit the spacecraft with a uniform supersonic speed in the radial (y) direction, which is hence the marching direction. New grid points are determined by the forward intersection of continuous C^+ (fan) characteristics with a new line $y = y_{new}$, whereas segments of the transverse C^- characteristic lines are reversely extended from each new grid point and require interpolation between old line grid points $(y = y_{old})$. This modified marching scheme is analogous to existing time dependent 1-D characteristics methods (see Sections 19-6(a) and 19-6(j) in [4]); however, we found no reference to the use of Riemann invariants as flow variables in a CRW computation in order to reduce interpolation errors.

The resulting SIMA scheme replicates a planar CRW (Prandtl-Meyer flow) exactly, lending an extra measure of credibility to its accuracy in computing a ring-symmetric CRW. For the new line segment lying outside the CRW, grid points are evenly distributed through the segment, and a fully inverse marching scheme is used. The SIMA scheme is described briefly in chapter 2 ; it was implemented in a FORTRAN code named "JET", which was specifically written for the computation of ring-jets having a vacuum background. A detailed description of the code JET and the finite difference schemes on which it is founded will be given in a future report [11] .

Our analytic approximation to a ring-symmetric CRW is formulated as follows. In a planar (Prandtl-Meyer) CRW the flow is uniform along the characteristic lines that fan out from the corner (we assume it is the C^+ family). In the ring-symmetric case the flow near the corner approaches asymptotically a corresponding planar CRW flow, which we term the *associate* CRW. However, the gradients along C^+ characteristics at the corner of a ring-symmetric CRW do not vanish as in a planar CRW. The key idea is thus : evaluate flow gradients in C^+ directions at the corner, then use them to extrapolate the associate CRW along C^+ lines to a finite distance from the corner. This extrapolation constitutes an approximation to the ring-symmetric CRW. Our present approach is analogous to the GRP (Generalized Riemann Problem) analysis from which high resolution upwind schemes for time dependent Euler equation were derived [5,6] . In terms of specific results, however, it is quite different from the original GRP analysis.

A perturbation approach to steady supersonic flow in two-dimensional space (plane or axial symmetry) using characteristic coordinates. has been developed by Ostwatitsch and colleagues [7]. Their work also included treatment of axisymmetric CRW. However, their approach is formulated in terms of small perturbation relative to a uniform supersonic flow. In our analysis the CRW is

assumed to span the range from some finite pressure to vacuum, and the perturbation scheme consists of regarding the axisymmetric terms in the governing equations as causing a small deviation from a Prandtl-Meyer flow. Our analytic approximation to a ring-symmetric CRW is presented in chapter 3 and Appendix A.

The present approach to the approximation of a ring-symmetric CRW can also be adapted to treat other axisymmetric centered waves, such as the divergent lip-centered CRW at an axisymmetric nozzle exit, or the cylindrically converging CRW at the base corner of an axisymmetric projectile moving at supersonic speed in air.

A series of computations were performed on a sample case of typical HF/DF laser exhaust. A comparison was made between results of numerical integration (SIMA) and the method of matched approximation to the ring-symmetric CRW . In particular, molecular opacity (expected number of collisions along a path of a fast penetrating molecule) was evaluated. Reasonable agreement between SIMA and approximated opacity was demonstrated. These results and their analysis are presented in chapter 4.

It seems that the present approach can be adapted to other problems calling for opacity of the CRW region in a ring-symmetric or axisymmetric exhaust plume.
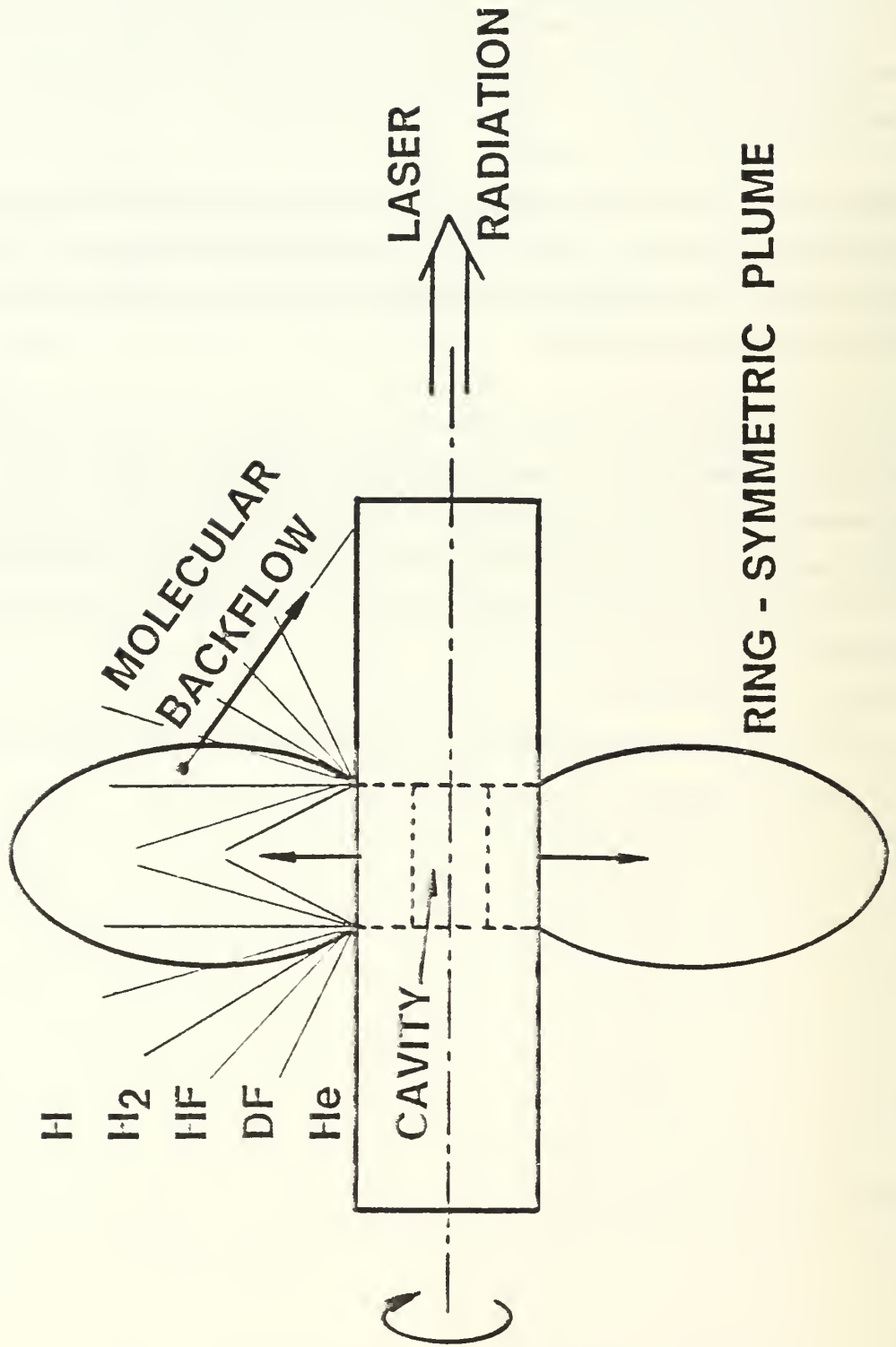
Figure 1-1.   Ring-Symmetric HF DF Laser Exhaust Plume

4

2.   THE FINITE DIFFERENCE SCHEMES FOR COMPUTING RING - JETS

The free expansion of a spacecraft exhaust plume is idealized in our study as a steady supersonic isentropic flow in two-dimensional axisymmetric coordinates, with a zero-pressure background. The most accurate finite difference scheme for this type of flow is the well known method of characteristics [8]. At an earlier phase of the present laser exhaust study, a code AXSYM [9] was written for the computation of ring-jet flow fields, using the direct method of characteristics. A notorious shortcoming of this method is that it yields the flow field at a set of grid points formed by the (oblique) intersection of the C^- and C^+ families of characteristic lines. The resulting grid is highly irregular (especially at regions of hypersonic flow), and it also requires the retention of grid-image matrices for the several regions formed by intersection of families of characteristic lines and their reflection from the mid-plane of symmetry ($x = 0$).

A commonly accepted remedy to these shortcomings is the inverse marching characteristic scheme [4]. The marching is in the downstream direction, i.e., the y direction in our case. The grid points are located on a succession of constant y rows, thereby introducing a measure of regularity in the solution grid. Computer memory requirements are drastically reduced : just two rows are kept in core memory - an "old" line of grid points and a "new" line of grid points. For reasons which will be elucidated below, the flow variables in our scheme are the Riemann invariants $(v \pm \theta)$. The integration of of the flow equations in characteristic form (sometimes referred to as compatibility relations [4]), is performed by a combination of two marching schemes. At grid points outside the CRW we use the conventional inverse marching scheme. At grid points within the CRW, we use a modified scheme named SIMA - Semi Inverse Marching Algorithm, tailored specifically to render accurate computation of a centered wave flow. In the sequel, we outline both schemes and describe the procedure by which they are combined to yield the flow field of a ring-symmetric jet. More information on the schemes and the code JET will be provided in a future report [11] .

The basic building block of both inverse and semi-inverse marching schemes is the evaluation of flow variables at a new grid point x_4 on the new line ($y = y_{new}$), given the flow at a row of grid points on the old line ($y = y_{old}$), which is initially the nozzle exit surface where flow is assumed uniform (Figure 2-1).

Consider first the inverse marching scheme (Figure 2-1a). The trace points x_1 , x_2 are determined by reversely extending C^- and C^+ characteristic lines from point (x_4, y_{new}) to the old line (Figure 2-1a). The characteristic segments are approximated by straight line segments, whose

slopes are initially taken from linearly-interpolated flow properties at the old point (x_4, y_{old}). Trace points x_1 and x_2 are assigned values of flow variables obtained by linear interpolation between their respective nearest-neighbor (old) grid points.

The compatibility relations along segments of C^- and C^+ characteristic lines in finite difference form are now solved, yielding the flow variables $(\nu \pm \theta)$ at the new grid point :

$$\text{Along } C^+ \quad \ldots \quad (\nu - \theta)_4 = (\nu - \theta)_2 + \omega \sin\mu_{24} \sin\theta_{24} \, \Delta\eta \, / \, y_{24}$$

$$(2\text{-}1)$$

$$\text{Along } C^- \quad \ldots \quad (\nu + \theta)_4 = (\nu + \theta)_1 + \omega \sin\mu_{14} \sin\theta_{14} \, \Delta\xi \, / \, y_{14}$$

Where $\Delta\xi$, $\Delta\eta$ are the length of the respective characteristic segments; indices 14, 24 refer to centered segment values obtained by averaging the values of variables at segment endpoints. The symmetry index ω is as follows : $\omega = 0$ for plane flow, $\omega = 1$ for axisymmetric flow. The usual isentropic relation [8] is used to determine μ from ν.

Equation (2-1) is now regarded as an implicit relation between the flow variables at the new grid point x_4 and the interpolated flow variables at the trace points x_1 and x_2. An updated pair of trace points is re-computed from an updated value of flow variables at the new grid point, and the procedure is repeated until convergence is established.

The Semi Inverse Marching Algorithm (SIMA) is a relatively simple modification of the inverse marching scheme. Rather than seek a solution on a new grid point x_4 whose location is unrelated to the row of old grid points, we determine x_4 by the forward extension of a C^+ characteristic line from an old grid point x_2 (Figure 2-1b). The trace point x_1 is determined by reversely extending the C^- characteristic line from the new grid point, just as in the inverse marching scheme. The same compatibility equation (2-1) is solved for the flow at the new grid point, except for an obvious geometrical modification : whereas in the inverse marching scheme the trace points x_1 and x_2 were re-computed in each iteration, the SIMA variant calls for re-computing the new grid point x_4 and the trace point x_1 until convergence is established.

The resulting scheme replicates a (planar) Prandtl-Meyer flow exactly. The reason for that is the combination of the semi-inverse marching idea with the choice of Riemann invariants as flow variables. Due to this choice, the compatibility relation along the fan characteristics (C^+) reduces to the exact relation $(\nu - \theta) = \text{constant}$. The equation along C^- still requires interpolation in old

values of $(v + \theta)$. However, in a C^+ Prandtl-Meyer flow $(v + \theta)$ is *uniformly constant,* so that interpolation does not introduce any truncation errors. It is noted that this feature is lost if any other flow variable is used in conjunction with a SIMA scheme for computing the flow in a CRW.

The boundary conditions are quite simple. Marching starts out from the nozzle exit surface where the flow is assumed uniform. The flow is bounded on the left by a mid-plane of symmetry $(x = 0)$, where the boundary condition is simply $\theta = 90°$. On the vacuum side we approximate the idealized zero-pressure background by terminating the computation at a high Mach number (fan) characteristic line (typically $M = 34$ at the corner). It is noted that as a result of ending the computation at a characteristic line, the total mass flow through a solution line y_{new} decreases slightly as y_{new} increases.

A sample computation performed by the code JET is displayed in Figure 2-2. The CRW region is clearly shown as bounded by the final C^+ characteristic line on the vacuum side, and by the leading C^+ characteristic and its reflection, on the other side. The code JET can also plot an assortment of special lines : characteristics, continuum breakdown lines [2], lines of constant Mach number, streamlines and lines of constant lateral molecular opacity (expected number of collisions by a fast molecule entering the plume in the x direction).
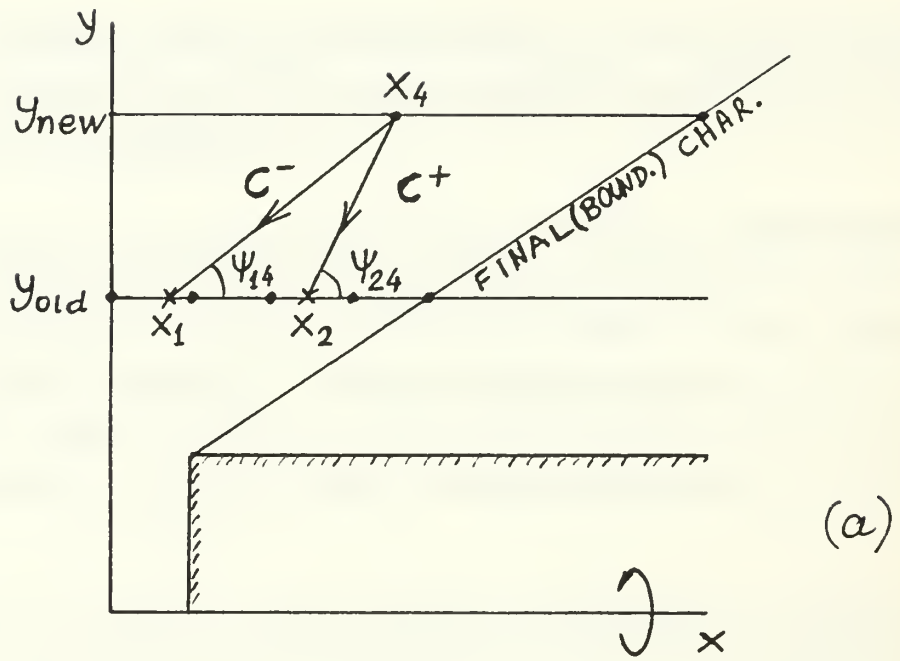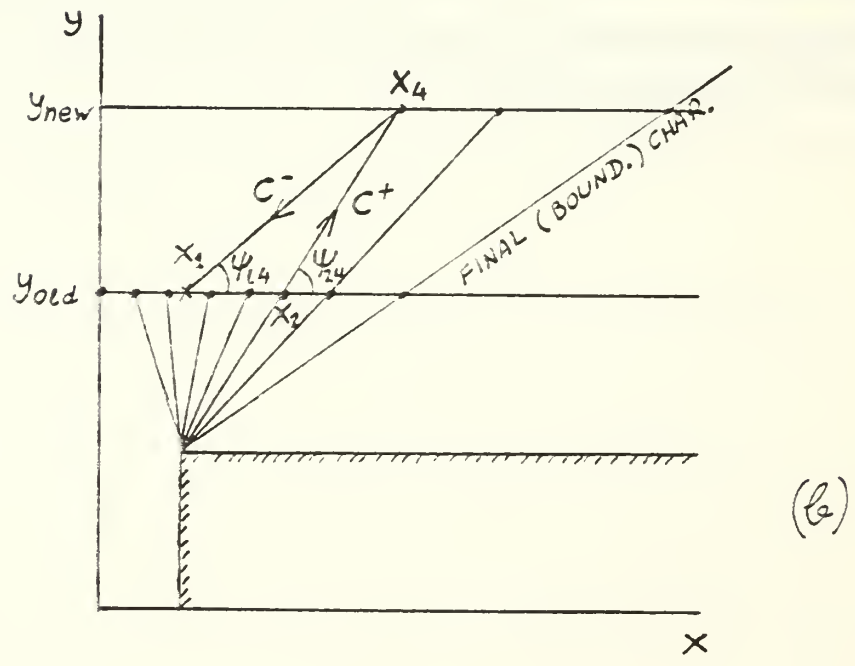
Figure 2-1.   Characteristic Marching Scheme for Supersonic Flow in Two Space Dimensions
(a) Inverse Marching   (b) Semi-Inverse Marching

8

Figure 2-2.   Ring-Symmetric Flow Field with Centered Rarefaction Wave

9

3. ANALYTIC APPROXIMATION OF RING-SYMMETRIC CENTERED RAREFACTION WAVES

The procedure for the analytic approximation of a ring-symmetric CRW comprises of two distinct phases. The first phase is an analysis of the flow field nea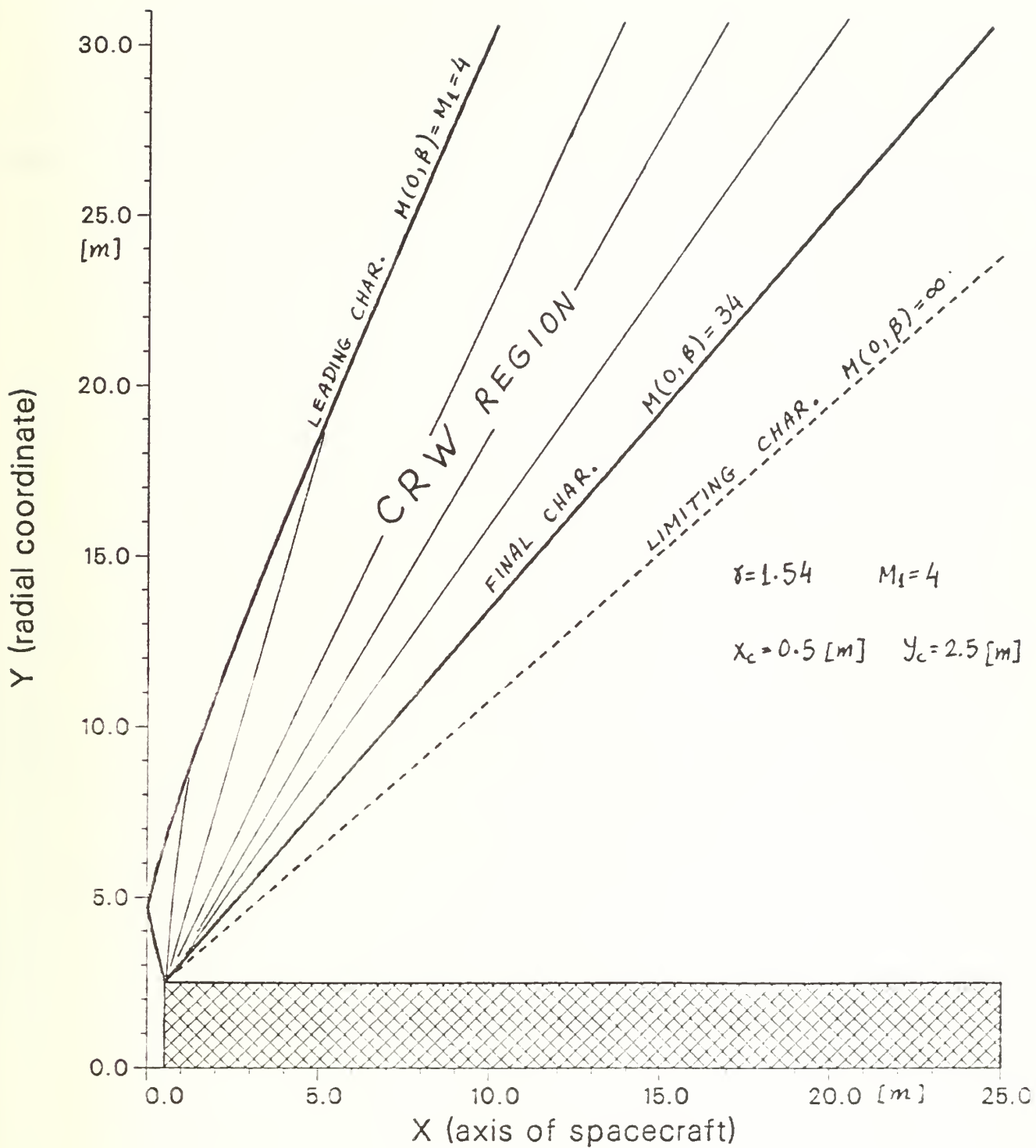r the corner of a ring-symmetric CRW, resulting in fan-wise gradients of flow variables at the corner. The second phase is an extrapolation of the *associate* CRW at the corner, using the fan-wise gradients obtained in the analytic phase. A concise description of each phase is given below, followed by a detailed presentation in sections 3.1, 3.2 and 3.3.

The first phase is an analysis of the flow near the corner of a ring-symmetric CRW. It is noted that in a planar C^+ CRW all directional derivatives of flow variables along C^+ vanish, but directional derivatives in any non C^+ direction increase beyond bound as the point at which they are evaluated approaches the corner. This suggests that the analysis of a ring-symmetric CRW as a perturbation of its associate CRW should be formulated *in characteristic coordinates*. The goal of this analysis would be to derive closed-form expressions for the C^+ directional derivatives of flow variables at the corner. A detailed presentation of the analytic phase is given in section 3.1 below.

In the second phase, the C^+ gradients at the corner are used to extrapolate the associate CRW at the corner to some finite distance along C^+ characteristic lines. It is this extrapolation that constitutes our analytic approximation to a ring-symmetric CRW. Rather than merely extend the associate CRW through linear extrapolation (i.e., a Taylor series truncated after the first-order term) using the corner C^+ derivatives, we opt for a specially formulated *"matched extrapolation"* scheme, where the extended flow field is matched to conform exactly to the flow along the pre-reflection segment of the leading characteristic $C^+(\beta_1)$. The result is a ring-symmetric CRW approximation that maintains reasonable accuracy levels up to several corner radii away from the corner – a considerably larger range of validity than that of a linear (unmatched) extrapolation. The matched extrapolation is described in section 3.2 below.

Finally we consider an "inverse problem" which is stated as follows. Given a point (x_0, y_0) within a ring-symmetric CRW, find the flow variables at this point. The matched extrapolation scheme is geared to deliver the flow field along *entire* C^+ characteristic lines (including the determination of the characteristic lines themselves in (x, y) coordinates). We do not know apriori the line C^+ passing through (x_0, y_0) , and we seek an algorithm for obtaining the flow at (x_0, y_0) without resorting to excessive numerical integrations. The solution to the inverse problem relies on the observation that C^+ lines are usually just slightly curved; it is presented in section 3.3 below.

3.1   Analysis of Ring-Symmetric CRW

Consider a 2-D axisymmetric steady inviscid flow of an ideal gas. If the flow is also supersonic, isentropic and irrotational, the governing equations in characteristic form using the Riemann invariants as flow variables [8] are :

$$\text{Along } C^+(\beta) \quad \ldots \ldots \quad (\nu - \theta)_\alpha = \sin\mu(\alpha,\beta) \, \sin\theta(\alpha,\beta) \, \eta_\alpha(\alpha,\beta) \,/\, y(\alpha,\beta)$$

$$\text{Along } C^-(\alpha) \quad \ldots \ldots \quad (\nu + \theta)_\beta = \sin\mu(\alpha,\beta) \, \sin\theta(\alpha,\beta) \, \xi_\beta(\alpha,\beta) \,/\, y(\alpha,\beta)$$

$$(3.1\text{-}1)$$

$$\text{Direction of } C^+(\beta) \quad \ldots \ldots \quad \psi(\alpha,\beta) = \theta(\alpha,\beta) + \mu(\alpha,\beta)$$

$$\text{Direction of } C^-(\alpha) \quad \ldots \ldots \quad \chi(\alpha,\beta) = \theta(\alpha,\beta) - \mu(\alpha,\beta)$$

where (α,β) are *the characteristic coordinates* , α being constant along $C^-(\alpha)$ and β being constant along $C^+(\beta)$. $\xi(\alpha,\beta)$ and $\eta(\alpha,\beta)$ are the distance (from an as yet unspecified origin) along C^- and C^+ respectively. We note that (ξ,η) *would not qualify as an alternate set of characteristic coordinates* , since in general ξ is not constant along C^+ and likewise η is not constant along C^-.

The specific definition of (α,β) , $\xi(\alpha,\beta)$ and $\eta(\alpha,\beta)$ is now tailored to the needs of the intended ring-symmetric CRW analysis. To fix ideas we consider a C^+ CRW : it is then natural to stipulate that $\alpha = 0$ and $\eta = 0$ at the corner. Denoting by index 1 the leading characteristic $C^+(\beta_1)$, we define the characteristic coordinates α and β as follows :

$$\alpha = \eta(\alpha,\beta_1)$$

$$(3.1\text{-}2)$$

$$\beta = M(0,\beta)$$

Where $M(0,\beta)$ is the Mach number at the associate CRW. We shall generally use β in lieu of $M(0,\beta)$, in order to simplify notation while maintaining the important distinction between the associate Mach number $M(0,\beta)$ and the Mach number within the ring-symmetric CRW $M(\alpha,\beta)$.

Let $Q(\alpha, \beta)$ denote any flow variable. We are seeking the corner gradient $Q_\alpha(0, \beta)$ in a ring-symmetric CRW. Since any flow variable Q can be expressed as function of $(v \pm \theta)$, Q_α can likewise be expressed in terms of $(v \pm \theta)$ and $(v \pm \theta)_\alpha$. Consequently, we should seek to derive expressions for $(v \pm \theta)_\alpha$ at $\alpha = 0$, from the governing equations (3.1-1). These equations are in a particularly simple form, in that only one Riemann invariant appears in each equation. Thus, the corner gradient $(v - \theta)_\alpha$ is already given by (3.1-1) upon setting $\alpha = 0$. We now turn to the derivation of $(v + \theta)_\alpha$.

A closed form expression for $(v + \theta)_\alpha$ can be derived from (3.1-1) as follows. Differentiate the equation along C^- characteristics with respect to α, set $\alpha = 0$ and then integrate the ensuing relation with respect to β, from the leading characteristic $C^+(\beta_1)$ to some internal characteristic $C^+(\beta)$. Since $C^-(\alpha)$ characteristic lines within the CRW shrink in size as α approaches zero, $\xi_\beta(0, \beta) = 0$. Hence, the only non zero term left for the β integration along $C^-(0)$ is the term containing $\xi_{\alpha\beta}(0, \beta)$. The result is the following expressions for $(v \pm \theta)_\alpha$ at the corner :

$$\left[(v - \theta)_\alpha\right](0, \beta) = \sin\mu(0, \beta) \, \sin\theta(0, \beta) \, \eta_\alpha(0, \beta) \, / \, y(0, \beta)$$

$$(3.1\text{-}3)$$

$$\left[(v + \theta)_\alpha\right](0, \beta) = \sin\mu(0, \beta_1) \, / \, y(0, \beta_1) + \left[y(0, \beta_1)\right]^{-1} \int_{\beta_1}^{\beta} \sin\mu(0, m) \, \sin\theta(0, m) \, \xi_{\alpha\beta}(0, m) \, dm$$

The boundary condition for the integration of $(v + \theta)_{\alpha\beta}$ was obtained by noting that along the leading characteristic $C^+(\beta_1)$:

$$\theta(\alpha, \beta_1) = \pi/2$$

$$\theta_\alpha(\alpha, \beta_1) = 0 \qquad\qquad\qquad (3.1\text{-}4)$$

$$(v - \theta)_\alpha = \sin\mu(\alpha, \beta_1) \, / \, y(\alpha, \beta_1)$$

We also note that at the corner $y(0, \beta) = y_c$ for any β. However, we shall maintain the notation $y(\alpha, \beta)$ and $y(0, \beta)$ in order to emphasize that $y(\alpha, \beta)$ is a field variable. The geometrical derivatives $\xi_{\alpha\beta}(0, \beta)$ and $\eta_\alpha(0, \beta)$ are readily derived from standard expressions of the associate CRW (Prandtl-Meyer flow, see Appendix A for details). They are given by :

12

$$\eta_\alpha(0,\beta) = \left\{ \left[1 + ((\gamma-1)/2)\beta^2\right] / \left[1 + ((\gamma-1)/2)\beta_1^2\right] \right\}^{(\gamma/2(\gamma-1))} \left\{ (\beta_1^2 - 1)/(\beta^2 - 1) \right\}^{1/4}$$

(3.1-5)

$$\xi_{\alpha\beta}(0,\beta) = ((\gamma+1)/4)\,\eta_\alpha(0,\beta)\,\beta^3\,(\beta^2 - 1)^{-1}\left[1 + ((\gamma-1)/2)\beta^2\right]^{-1}$$

Now, equations (3.1-3) and (3.1-5) constitute closed form expressions for the corner gradients $(\nu \pm \theta)_\alpha$. The only additional information needed is the standard Prandtl-Meyer expressions for $\theta(0,\beta)$ and $\nu(0,\beta)$ in the associate CRW (Appendix A). The integral in (3.1-3) cannot be expressed in terms of elementary functions ; however, it is readily evaluated by quadrature.

This concludes the analytic phase of the ring-symmetric CRW approximation. We now turn to the task of deriving closed-form expressions approximating the flow in a ring-symmetric CRW using the corner gradients $(\nu \pm \theta)_\alpha$.

3.2   The Matched Extrapolation Scheme

We seek an approximation to a ring-symmetric CRW that would be valid up to several corner radii from the corner. A direct substitution of the C^+ corner derivatives (3.1-3) in a Taylor series truncated after the first-order term, could be made. The result would be an expression where the local deviation of the ring-symmetric CRW from the corresponding associate CRW is proportional to $\Delta y = (y - y_c)$, i.e., a "linear extrapolation".

It turns out that in this case it is possible to formulate a *"matched extrapolation"* scheme, where the the aforementioned deviation depends nonlinearly on Δy, which would be consistent to first-order in $(\Delta y/y_c)$ with the corresponding linear extrapolation. This extrapolation is formulated to match exactly the flow along the leading characteristic $C^+(\beta_1)$. The advantage of this improved scheme is that it maintains better accuracy at $(\Delta y/y_c) = O(1)$ than the linear extrapolation, even though either scheme is formally first-order accurate near the corner.

The implementation of the matched scheme is effected through a change in flow variables from (ν,θ) to (f,θ) , where f is the streamtube area ratio function [8] , linked to the Prandtl-Meyer function and to the flow Mach number through the isentropic relations :

$$f = M^{-1} \left\{ (2/(\gamma+1)) \left[1 + ((\gamma-1)/2)M^2 \right] \right\}^{(\gamma+1)/2(\gamma-1)}$$

$$df/f = \left(M^2 - 1 \right)^{1/2} dv \tag{3.2-1}$$

$$dv = M^{-1} \left[1 + ((\gamma-1)/2)M^2 \right]^{-1} \left(M^2 - 1 \right)^{1/2} dM$$

We note that relations (3.2-1) hold in any steady flow where entropy is uniformly constant (homentropic flow). Thus, the *thermodynamic* flow variables M, f and v can be used interchangeably. The replacement of v by f is motivated by reasons which will be made clear in the sequel.

Let us find the expression for $f_\alpha(0,\beta)$. This is done by first eliminating $\theta_\alpha(0,\beta)$ by summing $(v+\theta)_\alpha$ and $(v-\theta)_\alpha$ in (3.1-3), obtaining an expression for $v_\alpha(0,\beta)$. Then, using the isentropic relations (3.2-1) to replace v_α by f_α and using (3.1-5) for $\eta_\alpha(0,\beta)$ and $\xi_{\alpha\beta}(0,\beta)$ we finally get :

$$f_\alpha(0,\beta) / f(0,\beta) = \delta(0,\beta) \, y_\alpha(0,\beta) / y(0,\beta)$$

$$\delta(0,\beta) = (1/2) \left\{ \left(\beta^2 - 1 \right)^{1/2} / \beta_1 \, \eta_\alpha(0,\beta) \sin\psi(0,\beta) \right\} +$$

$$(1/2) \left\{ \left(\beta^2 - 1 \right)^{1/2} \sin\theta(0,\beta) / \beta \sin\psi(0,\beta) \right\} + ((\gamma+1)/2(3-\gamma)) H(\beta) \tag{3.2-2}$$

$$H(\beta) = ((3-\gamma)/4) \left\{ \left(\beta^2 - 1 \right)^{3/4} \left[1 + ((\gamma-1)/2)\beta^2 \right]^{-\gamma/2(\gamma-1)} / \sin\psi(0,\beta) \right\} *$$

$$\int_{\beta_1}^{\beta} \left[1 + ((\gamma-1)/2)m^2 \right]^{(2-\gamma)/2(\gamma-1)} \left(m^2 - 1 \right)^{-5/4} m^2 \sin\theta(0,m) \, dm$$

where the specially defined function $H(\beta)$ has been normalized by a preceding factor so that $H(\infty) = 1$. A typical case of $H(\beta)$ is shown in Figure 3-1. By pre-computing (and storing) values of $H(\beta)$ as function of $1/\beta$ at a sequence of points (typically 50 points), $H(\beta)$ can readily be evaluated by linear interpolation.

14

Consider equations (3.2-2) at the leading characteristic $C^+(\beta_1)$. It is readily verified that $H(\beta_1) = 0$ and $\delta(0,\beta_1) = 1$. Consequently, equation (3.2-2) assumes the following form at the leading characteristic $C^+(\beta_1)$:

$$f_\alpha(0,\beta_1)/f(0,\beta_1) = y_\alpha(0,\beta_1)/y(0,\beta_1) \tag{3.2-3}$$

Now, along $C^+(\beta_1)$ the relation between f_α and y_α can be derived directly from the the equation along C^+ for $(v-\theta)_\alpha$ (equation (3.1-1)), since along $C^+(\beta_1)$ $\theta_\alpha = 0$, and v_α can be replaced by an "isentropically equivalent" expression containing f and f_α according to the isentropic relation (3.2-1). The result is the following differential relation which holds along the *entire* leading characteristic $C^+(\beta_1)$ of the ring-symmetric CRW:

$$f_\alpha(\alpha,\beta_1)/f(\alpha,\beta_1) = y_\alpha(\alpha,\beta_1)/y(\alpha,\beta_1) \tag{3.2-4}$$

This differential relation can be readily integrated, yielding $f(\alpha,\beta_1)/y(\alpha,\beta_1) = $ constant. Indeed, this result is consistent with the very definition of f as an area ratio function, since the flow crossing the leading characteristic $C^+(\beta_1)$ diverges with cylindrical symmetry.

The analogy between (3.2-3) and (3.2-4) is appealing. Can the first equation of (3.2-2) be recast in a form that would yield the exact relation (3.2-4) along $C^+(\beta_1)$, rather than the "linearized" relation (3.2-3)? Let us formally rewrite the first equation of (3.2-2) as if it were valid for any $\alpha \geq 0$; not just for $\alpha = 0$:

$$f_\alpha(\alpha,\beta)/f(\alpha,\beta) = \delta(\alpha,\beta)\left[y_\alpha(\alpha,\beta)/y(\alpha,\beta)\right] \tag{3.2-5}$$

Since $\delta(\alpha,\beta)$ is not known to us (indeed, it is *defined* by the preceding equation), we introduce the following assumption which constitutes the *key approximation* of our matched extrapolation scheme:

$$\delta(\alpha,\beta) \approx \delta(0,\beta) \tag{3.2-6}$$

Using this approximation, equation (3.2-5) is readily integrated, yielding a relation between f and y that does not explicitly involve the function $y(\alpha,\beta)$:

$$f(\alpha,\beta) = f(0,\beta)\left[y(\alpha,\beta)/y(0,\beta)\right]^{\delta(0,\beta)} \tag{3.2-7}$$

15

This is the matched extrapolation of the area function f ; it is consistent with the linear extrapolation of f near the corner as would be derived from (3.2-2), and it is exact along the leading characteristic $C^+(\beta_1)$. Does this matching assure a reasonable level of accuracy throughout the ring-symmetric CRW ? We defer the consideration of this question to chapter 4, where the subject of accuracy will be discussed in conjunction with comparison to finite-difference computations using the code JET.

Let us examine the range of variation of $\delta(0,\beta)$ (Figure 3-2). Along the leading characteristic $C^+(\beta_1)$ we have $\delta(0,\beta_1) = 1$, which corresponds to a cylindrically divergent flow. At high values of β the power $\delta(0,\beta)$ increases almost monotonically to $\delta(0,\infty) = 2/(3-\gamma)$. (It actually attains a maximum value slightly higher than $\delta(0,\infty)$ -- see Figure 3-2). Assuming that a dilute gas has a specific heats ratio $\gamma \leq (5/3)$, the maximum value of $\delta(0,\infty)$ for any dilute gas is $\delta(0,\infty) \leq (3/2)$, which corresponds to a power no larger than midway between the cylindrical power ($\delta = 1$) and the spherical power ($\delta = 2$).

The power-law form of approximation (3.2-7) to streamtube area ratio in a ring-symmetric CRW suggests the following geometrical interpretation.

(a)   Consider the variation of area ratio along a particular streamtube. It consists of the product of two factors : the "planar CRW" area ratio $f(0,\beta)$ and a *radial divergence* factor. where the radial power is function only of β . There is some form of separation of variables in (3.2-7). $f(0,\beta)$ and $\delta(0,\beta)$ depend only on β which designates a characteristic line $C^+(\beta)$. The radial divergence factor involves y which designates points on $C^+(\beta)$. This is a direct consequence of our key assumption (3.2-6).

(b)   Consider the spacing between streamlines in the (x,y) plane of a ring-symmetric CRW. They are stretched by a factor $(y/y_c)^{\delta(0,\beta)-1}$ relative to corresponding streamlines in an otherwise identical planar CRW. The stretching power vanishes at the leading characteristic $C^+(\beta_1)$ and increases to an asymptotic value of $(\gamma-1)/(3-\gamma)$ as β increases to infinity.

(c)   At very large distance from the corner. one would expect streamtube cross-section area to exhibit spherical divergence. i.e. for a certain streamtube f should increase as y^2 . regardless of the value of γ . The fact that our power-law approximation does not exhibit these features indicates that it is an intermediate-range fit to the radially divergent CRW flow. Can a matching scheme between the intermediate-range and the far-range flow regimes be formulated? This question is presently an open one.

Any flow variable linked isentropically to $f(\alpha,\beta)$ can now be evaluated from the approximation (3.2-7). The "kinematic" variable $\theta(\alpha,\beta)$, however, is not related to $f(\alpha,\beta)$ in this manner, so its approximation is still pending.

A matched extrapolation scheme for $\theta(\alpha,\beta)$ is now formulated in a manner consistent with the scheme for $f(\alpha,\beta)$. This is done by regarding equation (3.1-1) along $C^+(\beta)$ as defining a differential relation between $\theta(\alpha,\beta)$ and $y(\alpha,\beta)$, since the differential relation between $v(\alpha,\beta)$ and $y(\alpha,\beta)$ can be eliminated by virtue of (3.2-5) and the isentropic relation between v and f given in (3.2-1). The result is a differential relation for $\theta(\alpha,\beta)$ along $C^+(\beta)$ analogous to the relation (3.2-5) for $f(\alpha,\beta)$:

$$\theta_\alpha(\alpha,\beta) = \varepsilon(\alpha,\beta)\left[y_\alpha(\alpha,\beta)/y(\alpha,\beta)\right]$$

$$\text{(3.2-8)}$$

$$\varepsilon(\alpha,\beta) = \delta(\alpha,\beta)\tan\mu(\alpha,\beta) - \sin\mu(\alpha,\beta)\sin\theta(\alpha,\beta) / \sin\psi(\alpha,\beta)$$

Now we invoke the same argument that lead to the key approximation (3.2-6), namely, that $\varepsilon(\alpha,\beta)$ may be replaced by its associate CRW value $\varepsilon(0,\beta)$. Hence, the matched extrapolation for $\theta(\alpha,\beta)$ is given by :

$$\theta(\alpha,\beta) = \theta(0,\beta) + \varepsilon(0,\beta)\ln\left[y(\alpha,\beta)/y(0,\beta)\right]$$

$$\text{(3.2-9)}$$

$$\varepsilon(0,\beta) = \delta(0,\beta)\tan\mu(0,\beta) - \sin\mu(0,\beta)\sin\theta(0,\beta) / \sin\psi(0,\beta)$$

Let us examine the function $\varepsilon(0,\beta)$ (Figure 3-3). We observe that $\varepsilon(0,\beta_1) = 0$ in accordance with the boundary condition at the leading characteristic $C^+(\beta_1)$: $\theta_\alpha(\alpha,\beta) = 0$. (Since by (3.2-8) $\varepsilon(\alpha,\beta_1) = 0$ for any α, this boundary condition cannot be considered as a guideline in improving the $\theta(\alpha,\beta)$ extrapolation as was the case with the $f(\alpha,\beta)$ extrapolation). At large β : $\delta(0,\beta) \to 2/(3-\gamma)$, so that $\beta\varepsilon(0,\beta) \to (\gamma-1)/(3-\gamma)$. Consequently, the effect of ring symmetry is to deflect streamlines toward the radial direction (y) relative to their associate CRW direction, by an amount that decreases in the hypersonic portion of the CRW, as the inverse of the associate Mach number.

An unexpected difficulty arises when the logarithmic extrapolation (3.2-9) for $\theta(\alpha,\beta)$ is considered for large $y(\alpha,\beta)$. At some sufficiently large $y(\alpha,\beta)$, $\theta(\alpha,\beta)$ will exceed $\pi/2$, which seems physically unrealistic. A possible remedy would be to replace (3.2-9) by a modified extrapolation obtained as follows. Multiply (3.2-8) by $\tan\theta(\alpha,\beta)$, and invoke the modified approximating

assumption that $\varepsilon(\alpha,\beta)\,\tan\theta(\alpha,\beta)$ may be replaced by $\varepsilon(0,\beta)\,\tan\theta(0,\beta)$. Since $d(\tan z) = -\,d(\ln(\cos z))$, the result is the following power-law extrapolation :

$$\cos\theta(\alpha,\beta) \;=\; \cos\theta(0,\beta)\,\big[y(\alpha,\beta)/y(0,\beta)\big]^{-\kappa(0,\beta)}$$

$$\text{(3.2-10)}$$

$$\kappa(0,\beta) \;=\; \varepsilon(0,\beta)\,\tan\theta(0,\beta)$$

We notice that by this power-law approximation $\theta(\alpha,\beta)$ cannot exceed $\pi/2$. Also, in applying (3.2-10) care should be exercised near $\beta = \beta_1$, since $\kappa(0,\beta_1)$ is singular. However, a simple analysis shows that $\kappa(0,\beta)$ approaches a finite limit at β_1, which can be expressed in closed form, and since $\cos\theta(0,\beta_1) = 0$ the boundary condition $\cos\theta(\alpha,\beta_1) = 0$ is fulfilled regardless of the value of $\kappa(0,\beta_1)$. The power $\kappa(0,\beta)$ for a typical case is shown in Figure 3-4.

One more variable is needed to complete the approximation to the ring-symmetric CRW : the $C^+(\beta)$ characteristic direction $\psi(\alpha,\beta)$. It is simply given by :

$$\psi(\alpha,\beta) \;=\; \theta(\alpha,\beta) \;+\; \mu(\alpha,\beta)$$

$$\text{(3.2-11)}$$

where $\theta(\alpha,\beta)$ is given by either (3.2-9) or (3.2-10). The Mach angle $\mu(\alpha,\beta)$ is obtained from $f(\alpha,\beta)$ through the isentropic relation (3.2-1), where $f(\alpha,\beta)$ is given by the approximation (3.2-7).

This concludes the specification of a ring-symmetric CRW through matched extrapolation of the associate CRW. To obtain the flow field of a particular ring-symmetric CRW, one integrates the relation defining $C^+(\beta)$, i.e., $dx = \cot\psi\,dy$, while evaluating the flow variables using the aforementioned approximations. The result is flow field information at a series of points (x,y) along $C^+(\beta)$ characteristic lines.

There remains one more approximation task : the "inverse problem", which is stated as follows. Given a point (x_0,y_0) in the ring-symmetric CRW, trace "inversely" the characteristic line through it, and hence find the flow variables solely at (x_0,y_0), using the matched extrapolation scheme. An efficient method for resolving the inverse problem is described in section 3.3 below.

18

3.3 The Inverse Problem

Consider the following application of the present approximation to a ring-symmetric CRW. A physical model is related to the flow in a ring-symmetric CRW. The computation scheme of that model requires flow variables at a large number of points (x_0, y_0) within the flow field. The implementation of such a model calls for an efficient algorithm capable of providing flow variables at points (x_0, y_0), without resorting to computation of the flow at a surrounding cluster of points, or along a set of adjacent characteristic lines.

It is observed that through all but the low supersonic portion of a ring-symmetric CRW, the C^+ characteristics are nearly straight lines. This suggests the following approximation procedure for the inverse problem. Assume as a first guess that $C^+(\beta)$ through point (x_0, y_0) is a straight line; then correct the resulting value of β by finding the small deviation of $C^+(\beta)$ from a straight line, using a linearized approximation to $\psi(\alpha, \beta)$.

To do that we need a closed-form expression for $\psi(\alpha, \beta) - \psi(0, \beta)$. The implicit definition (3.2-11) will not be adequate. Instead, we seek an extrapolation scheme formulated directly for $\psi(\alpha, \beta)$. Following a procedure analogous to that by which the $f(\alpha, \beta)$ and $\theta(\alpha, \beta)$ approximations were obtained, we get :

$$\psi_\alpha(\alpha, \beta) = \lambda(\alpha, \beta) \left[y_\alpha(\alpha, \beta) / y(\alpha, \beta) \right]$$

$$\lambda(\alpha, \beta) = \varepsilon(\alpha, \beta) - \delta(\alpha, \beta) \left[1 + ((\gamma-1)/2) M^2 \right] \left(M^2 - 1 \right)^{-3/2} \qquad (3.3\text{-}1)$$

$$M = M(\alpha, \beta)$$

Again we invoke the argument that (3.3-1) is exact, but it involves the unknown functions $\varepsilon(\alpha, \beta)$, $\delta(\alpha, \beta)$ and $M(\alpha, \beta)$, so that they ought to be approximated by their respective associate functions, i.e., $\varepsilon(0, \beta)$, $\delta(0, \beta)$ and $M(0, \beta)$. (We might have retained the Mach number as $M(\alpha, \beta)$ and approximate it through (3.2-7) ; however, that would have made it impossible to obtain a closed-form expression for the ensuing y-integration). Thus, replacing $\lambda(\alpha, \beta)$ by $\lambda(0, \beta)$, we get :

19

$$\psi(\alpha,\beta) - \psi(0,\beta) = \lambda(0,\beta) \ln[y(\alpha,\beta)/y(0,\beta)]$$

(3.3-2)

$$\lambda(0,\beta) = \varepsilon(0,\beta) - \delta(0,\beta) \left[1 + ((\gamma-1)/2)\beta^2\right] (\beta^2 - 1)^{-3/2}$$

The unknown β_0 is now to be determined by solving the equation :

$$x_0 = x_c + \int_{y_c}^{y_0} \cot\psi(\alpha,\beta_0) \, dy(\alpha,\beta_0)$$

(3.3-3)

To get an explicit solution for β_0 from (3.3-3), we "linearize" this equation by letting :

$$\cot\psi(\alpha,\beta_0) \approx \cot\psi(0,\beta_0) - \left[\psi(\alpha,\beta) - \psi(0,\beta_0)\right] / \sin^2\psi(0,\beta_0)$$

(3.3-4)

We substitute this approximation in (3.3-3) and we use the expression (3.3-2) for $\psi(\alpha,\beta)$. The y integration can then be performed in closed form, yielding the following equation for β_0 :

$$\cot\psi(0,\beta_0) = (x_0 - x_c) / (y_0 - y_c) +$$

$$\left[y_0 \ln(y_0/y_c) / (y_0 - y_c) - 1\right] \left[\lambda(0,\beta_0) / \sin^2\psi(0,\beta_0)\right]$$

(3.3-5)

When $\lambda(0,\beta_0)$ is sufficiently small, (3.3-5) can be solved for β_0 by repeatedly computing β_0 on the left side using a former iteration value of β_0 on the right side. In this procedure, we also use the associate CRW relation between $\psi(0,\beta_0)$ and β_0 (see Appendix A). For the initial iteration we set $\lambda(0,\beta_0) = 0$.

The accuracy of solving the inverse problem is not as good as that of the direct matched extrapolation. Additional errors are generated by the linearization (3.3-4) and also by the approximation (3.3-2) to $\psi(\alpha,\beta)$ which is inferior to (3.2-11). Thus, along the leading characteristic $C^+(\beta_1)$ the direct approximation becomes exact, but the inverse procedure remains an approximation.

The coefficient $\lambda(0,\beta)$ is usually fairly small (Figure 3-5). For large β the following asymptotic expression is readily found from (3.3-2) : $\beta\lambda(0,\beta)\to 0$, so that the accuracy of the inverse procedure improves as (x_0,y_0) moves into the hypersonic portion of the ring-symmetric CRW. If this accuracy is inadequate when (x_0,y_0) is near $C^+(\beta_1)$, we can revert to solving (3.3-3) for β_0 by some iterative scheme, performing the integration along $C^+(\beta_0)$ numerically, while using the better approximation (3.2-11) for $\psi(\alpha,\beta_0)$. Naturally, this procedure would entail a much higher expenditure of CPU time than the approximation (3.3-5).

For the sake of completeness, there is one more point to discuss in regards to the inverse problem. When the iterative procedure of Eq. (3.3-5) involves values of β_0 sufficiently close to the value β_1 of the leading characteristic, a difficulty may arise. The reason is that while the leading characteristic is exactly replicated by the matched approximation, the "linearized" approximation to the leading characteristic (obtained by computing x_0 as function of y_0 from Eq. (3.3-5) with $\beta_0=\beta_1$), curves towards the interior of the CRW. This situation is depicted in Figure 3-6. Thus, the iteration procedure of Eq. (3.3-5) would come up with a tentative solution having $\beta_0 < \beta_1$ for points (x_0,y_0) located between the exact and approximate leading characteristics (shaded area in Figure 3-6), which is inconsistent since the range of acceptable values within the CRW is $\beta_0 > \beta_1$. The remedy is simply to set $\beta_0=\beta_1$ as the approximate solution to any point (x_0,y_0) within that "shaded area". To illustrate the magnitude of error introduced by this simplification, we show in Figure 3-6 the characteristic corresponding to $\beta=4.1$ (versus $\beta_1=4$). This difficulty, however, is probably of no concern to ambient scattering applications, since ambient molecules are typically stopped at the outer fringes (hypersonic portion) of the ring-symmetric CRW.
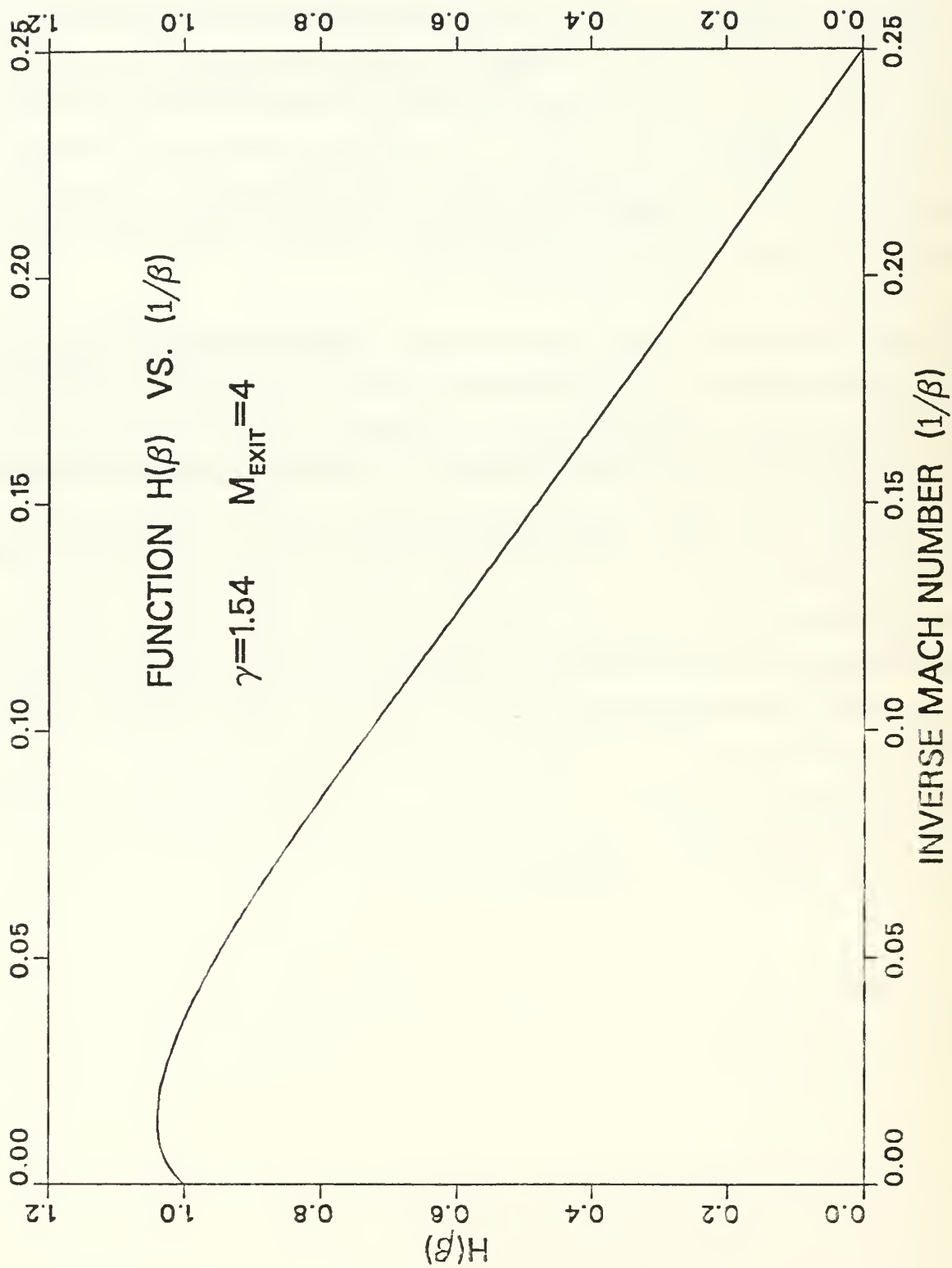
Figure 3-1. The Integral Function H(β) as Function of Inverse Mach Number

22
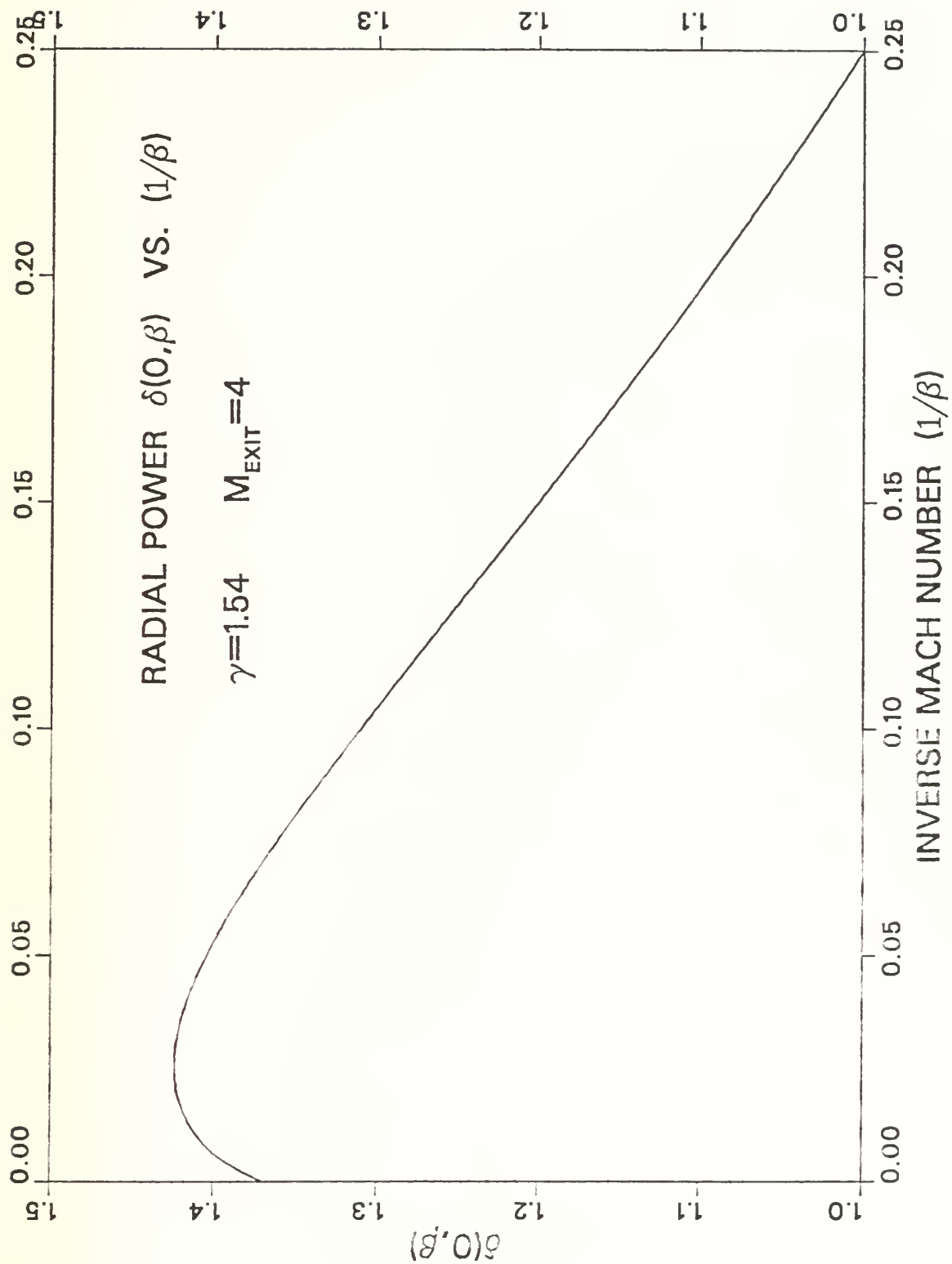
Figure 3-2.   Radial Power for Area Ratio as Function of Inverse Mach Number
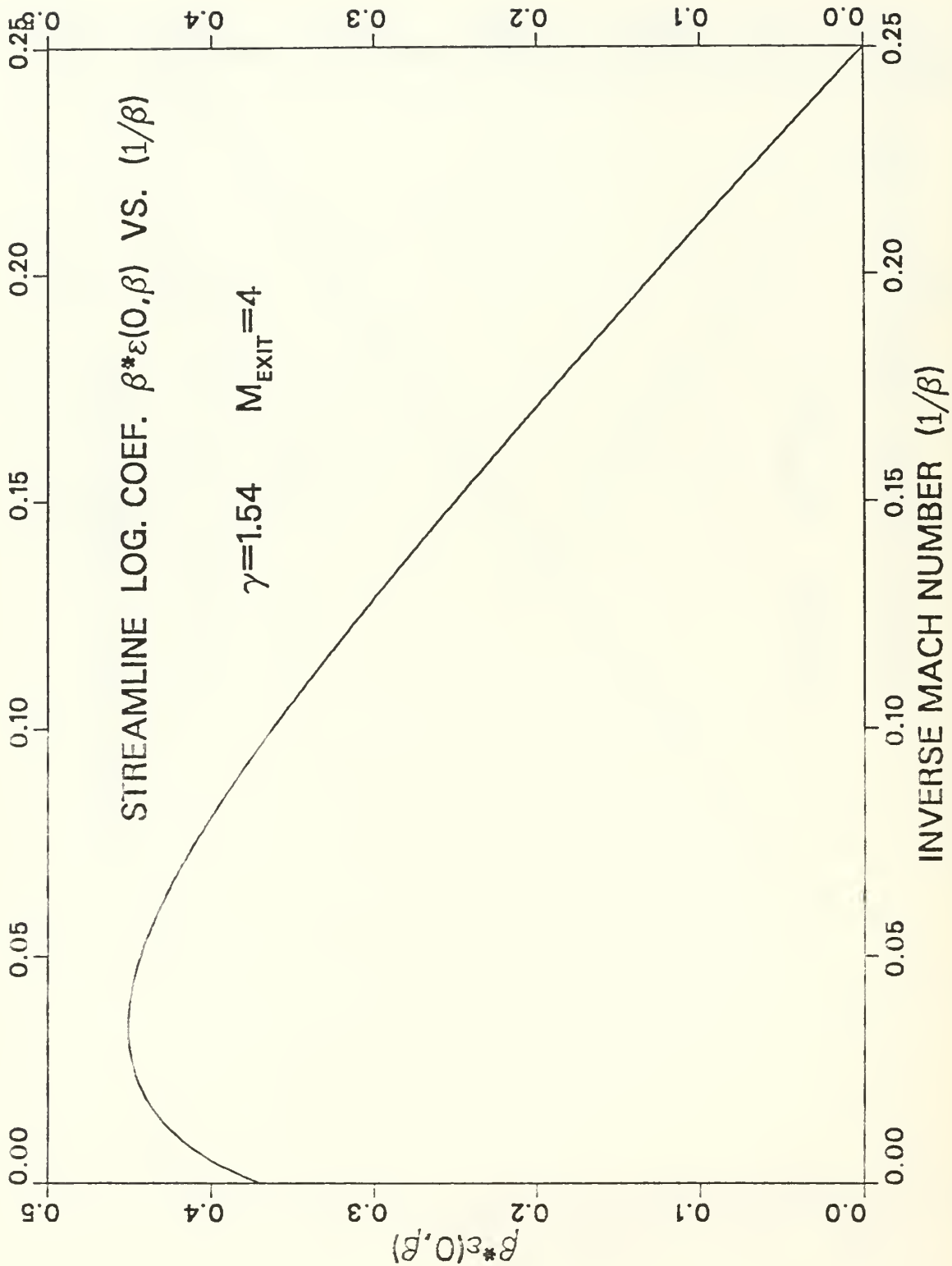
Figure 3-3. Coefficient of Logarithmic Variation in Flow Angle as Function of Inverse Mach Number
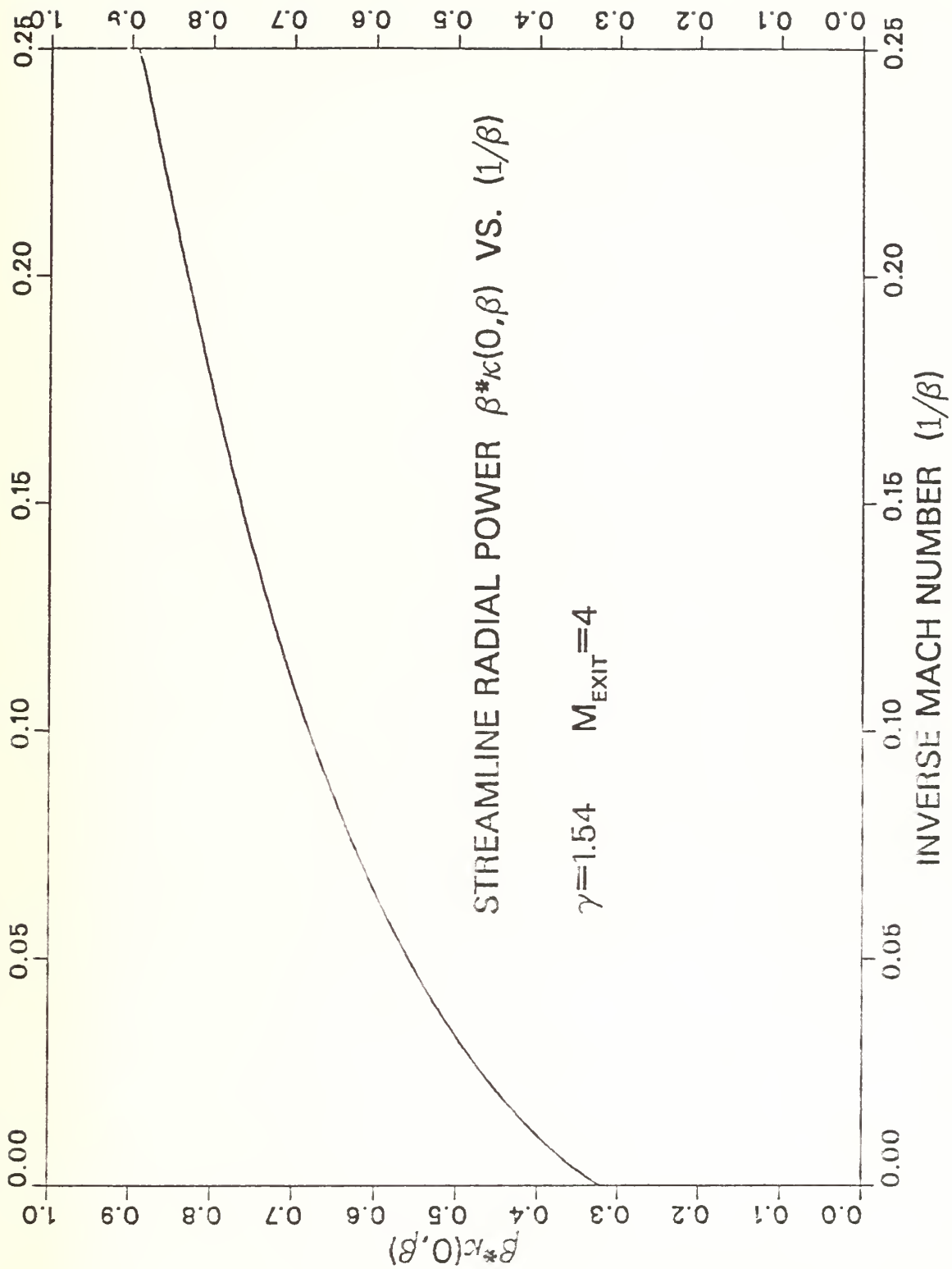
Figure 3-4.   Radial Power for Cosine of Flow Angle as Function of Inverse Mach Number
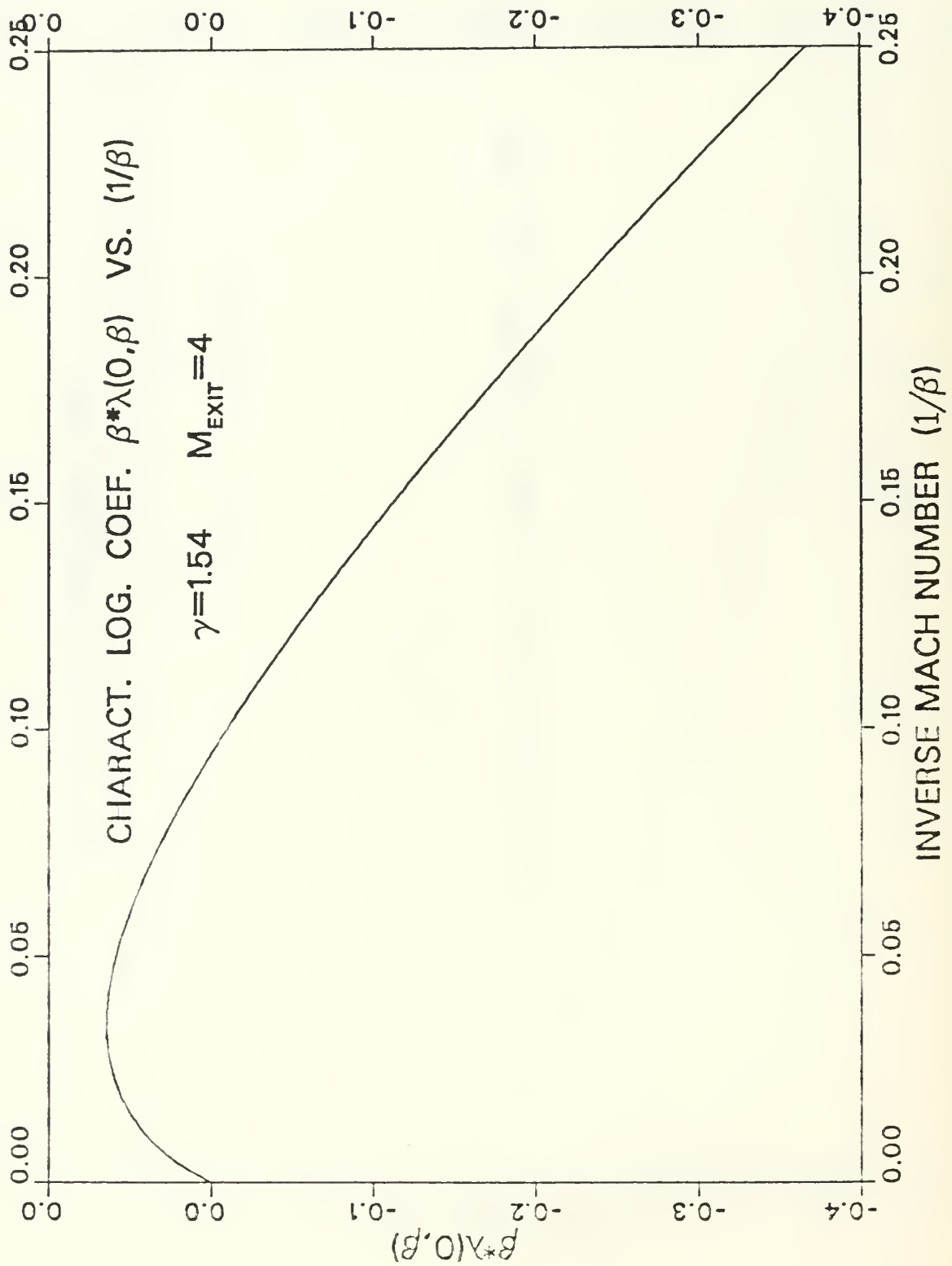
25

Figure 3-5. Coefficient of Logarithmic Variation in characteristic Angle as Function of Inverse Mach Number

26
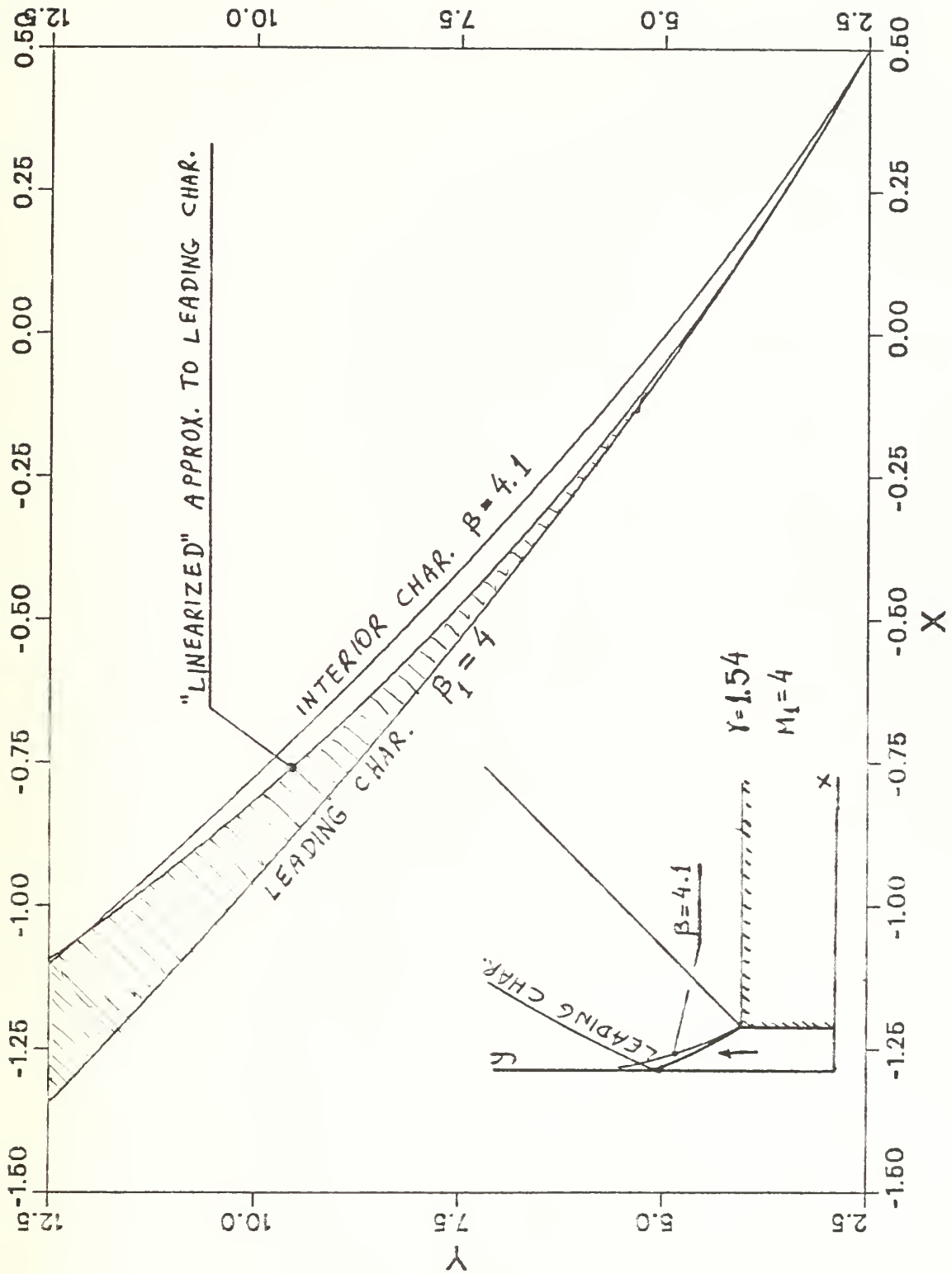
Figure 3-6.   Characteristic Lines Extended from Corner, Demonstrating the "Gray Area" between Exact and Linearized Leading Characteristics

27

4. RESULTS AND DISCUSSION

We now present computational results intended to exhibit some relevant features of ring-symmetric supersonic jets, and to demonstrate the nature of our matched approximation to the CRW region of the ring-jet flow field. A typical case of HF/DF laser exhaust was chosen [1,10] for these sample computations. It is specified in Table 4-1 below.

Table 4-1. Typical Operating Conditions of HF/DF Laser Exhaust

Mole fractions	[H] = .091 [HF] = .091 [H$_2$] = .104
	[DF] = .135 [He] = .579
Average molecular weight	7.27
Specific heats ratio	1.54
Stagnation temperature and density	2300 (K) and .0075 (kg/m^3)
Exit Mach number	4.0
Molecular diameter (hard spheres)	2.5x10^{-10} (m)
Spacecraft diameter	2.5 (m)
Aperture of ring-nozzle	1.0 (m)

4.1   Finite Difference Computation of Ring-Symmetric CRW

An accurate finite difference computation of the entire ring-symmetric CRW flow field was performed by the code JET utilizing the SIMA scheme (Ch. 2). A brief description of the computational procedure is now presented. Referring to Figure 4-1, the y marching step started at 0.01 (m) and was subsequently limited to half the step determined by the closest forward intersection of pairs of $C^{\pm}$ characteristics extended from adjacent grid points. At the outset, the number of lateral (x) grid intervals was 100, of which 60 were in the CRW and 40 spanned the nozzle exit. SIMA scheme was applied to all CRW grid points which were determined by a fan of C^{+} characteristic lines indexed from k = 1 (leading) to k = 61 (final). These fan lines were chosen to have equally spaced values of the Riemann invariant $(\nu - \theta)$ at the corner. The flow at all remaining grid points was computed via the inverse marching scheme (Ch. 2).

As the marching progressed, the leading characteristic (k = 1) approached the mid-plane of symmetry (x = 0) and it became necessary to switch the first SIMA-computed characteristic to k = 2, then subsequently to k = 3 and so on, until at y = 24 (m) it reached the index k = 19 (Figure 4-1). The result is that in addition to the region designated as CRW (Figure 2-2), also the region roughly coinciding with the open triangle between k = 19 on the left and the reflected characteristic k = 1 on the right, was computed via the SIMA scheme.

4.2   Continuum Breakdown

In a source-like flow of dense gas exhausting into vacuum, a breakdown of continuum flow inevitably takes place at some point along each streamtube [2]. In a planar CRW (Prandtl-Meyer flow), the breakdown surface approaches asymptotically a particular streamline as the distance from the corner increases [3,10]. However, in a ring-symmetric CRW the breakdown surface curves towards the mid-plane of symmetry, reaching it at some finite radius. Two breakdown surfaces were traced in the JET computation, corresponding to the plausible values of the breakdown parameter B = 0.05 and B = 0.08 ; they are shown in Figure 4-2. It is evident from this figure that most of the ring-symmetric CRW lies *outside* the breakdown surface.

Moreover, consider ambient scattering by molecules entering the CRW in the x direction. Most of these molecules will be stopped within a range for which the expected number of collisions with exhaust molecules is $\tau \approx 1$. In Figure 4-3 we show the line $\tau = 1$ plotted from the JET computation

of the typical laser exhaust (Table 4-1). It is clear that virtually all ambient scattering will take place outside the breakdown surface. Our model for estimating the molecular backflow induced by ambient scattering, relies on the presumption that continuum flow holds throughout the rarefaction fan, even at regions of near-vacuum. How can that approach be justified in view of the preceding discussion?

Consider a spherical source flow into vacuum [2], where the breakdown surface is in a region of hypersonic flow. A special situation in regards to continuum breakdown exists in this idealized case. The breakdown in continuum flow is first manifested by the failing of local temperature to adhere to the isentropic relation with local density. In fact, "temperature" ceases to exist, since the random component of molecular velocity does no longer have the (isotropic) Boltzmann distribution. By contrast, conservation of mass holds regardless of continuum flow breakdown, so that by virtue of the spherical symmetry, density decreases as $1/R^2$ to arbitrarily large R.

As demonstrated by Bird's Monte Carlo simulation of a Prandtl-Meyer flow [3], an analogous situation exists also in this self-similar flow field : the density follows quite closely the continuum (self similar) solution, even in regions well downstream from points where the isentropic relation between temperature and density has broken down. Since only density and flow velocity are needed in order to estimate ambient scattering (see [1], in particular the "cold" assumption), the foregoing discussion provides a justification for the use of continuum flow approximation to this end.

4.3   The Matched Approximation

Consider a particular characteristic line ($k = 47$) in the sample case computation (Figure 4-1). We focus on the variation of the three thermodynamic variables f (area ratio), M (Mach number) and v (Prandtl-Meyer function), along this characteristic line. These variables were computed via both the SIMA scheme (Ch. 2) and the matched approximation, and the results are shown in Figures 4-4, 4-5 and 4-6. As expected, Mach number and area ratio both increase along the characteristic line, due to the radial divergence of the flow. How well is this variation predicted by our matched approximation?

The matched approximation for thermodynamic variables is the radial power-law expression for the area ratio (3.2-7). M and v are computed from f via the standard isentropic relations. The following features are observed regarding the nature of the matched approximation in this sample case (Figures 4-4, 4-5 and 4-6).

(a)   Both SIMA and matched approximation curves start out with equal corner gradients. This constitutes a mutual validation for both the numerical integration scheme and the analytic approximation, in the vicinity of the corner.

(b)   The approximated f (Figure 4-4) is undervalued, resulting in a correspondingly undervalued Mach number (Figure 4-5). Had we opted for a linear extrapolation of f from the corner along fan characteristics, it is evident from Figure 4-4 that f would have been even more undervalued, and so would be the Mach number. Matched approximation is thus demonstrated to be clearly superior in accuracy to linear extrapolation.

(c)   What would be the quality of an approximation based on a linear extrapolation of v ? Using this variable would be consistent with the fact that the analytic expression of fan-wise gradients (3.1-3) is for gradients of the Riemann invariants.

From Figure 4-6 it is evident that a linearly extrapolated v would be grossly overvalued, while the matched approximation for v is moderately undervalued. A linear extrapolation of v would thus result in a grossly overvalued Mach number. (In fact, from Figure 4-6 it can be estimated that this would result in M reaching infinity around $y/y_c = 4$). This observation is not inconsistent with (b) above, as may seem at first. The isentropic relations between f, M and v are highly nonlinear, so that the quality of an approximation scheme depends on the particular thermodynamic variable chosen to be approximated (while the others are evaluated from the isentropic relations). The observation that a linear extrapolation of v would be a poor choice of approximation scheme, thus provides yet another support to the choice of f as the thermodynamic variable to be approximated.

Can any statement be made at this point about the level of accuracy of matched approximations to ring-symmetric CRW ? Discussing this question is contingent upon specifying some physical feature of the flow field for which a comparison will be made. Merely computing a flow variable, such as Mach number, does not constitute a meaningful test.

For the application which motivated the present study, namely ambient scattering, a meaningful feature of the flow field would be the cumulative number of collisions that a fast moving molecule entering the CRW from a bordering cavitation region, can expect. This quantity is path-dependent, so as a simplification we consider only rays parallel to the x axis (constant y). The number of collisions expected by a molecule reaching point (x_0, y_0) is :

$$\tau(x_0, y_0) = \int_{x_L}^{x_0} \sigma\, n(x, y_0)\, dx \qquad (4.3\text{-}1)$$

Where n is the number density, σ is the collision cross-section and x_L corresponds to the limiting characteristic. We generally assume hard-sphere collisions so that σ is a constant, and the "molecular opacity" τ is essentially a mass integral multiplied by σ.

The molecular opacity $\tau(x_0, y_0)$ was computed along with the computation of the flow field by the code JET. Some lines of constant opacity were traced; two of them are shown in Figure 4-3. The opacity in the CRW region was also computed from the matched approximation; the results compare well with those of SIMA computations, as can be seen in Figures 4-7 and 4-8. The method by which $\tau(x_0, y_0)$ was evaluated from the matched approximation is not a numerical integration. Rather, it is a closed-form approximation which we now proceed to describe.

Referring to Figure 4-9, the law of conservation of mass along a particular streamtube is used to establish the following relation between flow variables at points S on the characteristic line passing through (x_0, y_0) and points x on the segment $y = y_0$:

$$n(S)\, u(S)\, \sin\mu(S)\, y(S)\, \Delta S = n(x)\, u(x)\, \sin\theta(x)\, y_0\, \Delta x \tag{4.3-2}$$

The opacity integration (4.3-1) can thus be replaced by an integration along the characteristic line from (x_c, y_c) to (x_0, y_0). Now, some further simplifications are introduced, enabling a closed-form integration for the opacity. First we assume that the entire region of interest is one of very high Mach number, so that $1 + ((\gamma-1)/2)M^2 \approx ((\gamma-1)/2)M^2$. Powers of M can be approximately replaced by appropriate powers of f. We also assume that ψ and θ do not vary greatly through the region of interest, so that both can be reasonably well approximated by their corner values. Using the power law (3.2-7), the opacity integration is then readily performed, yielding the following expression:

$$\tau(x_0, y_0) = G(0, \beta_0)\, (y_0/y_c)^{-1} \left[(y_0/y_c)^{2 - \delta(\gamma+1)/2} - 1 \right] / [2 - \delta(\gamma+1)/2]$$

$$G(0, \beta_0) = \sigma\, n(0, \beta_0)\, y_c / M(0, \beta_0)\, \sin\theta(0, \beta_0)\, \sin\psi(0, \beta_0) \tag{4.3-3}$$

$$\delta = \delta(0, \beta_0) \qquad \text{(see Eq.(3.2-2) above)}$$

The opacity distributions shown in Figures 4-7 and 4-8 were computed from this expression. They compare favorably with SIMA opacities, demonstrating that for our purpose the matched approximation is reasonably accurate. In these JET computations the opacity at points on the

boundary (final) characteristic line was estimated from Eq. (4.3-3). The value of the boundary opacity represnts the effective thickness of the "missing" layer of fluid due to terminating the numerical computation at the characteristic having $M(0,\beta) = M_f$. The maximum value of this boundary opacity in the typical case was found to be about 0.16 (at $y/y_c = 3.2$ as in Fig. 4-7). This relatively low value indicates that as far as the interaction with invading ambient molecules is concerned, the final Mach number $M_f = 34$ is a reasonable substitute for $M_f = \infty$.

We observe that Eq.(4.3-3) predicts that opacity generally peaks at some point along each characteristic line (due to its particular dependence on y), which in the case shown in Figure 4-8, is confirmed by the SIMA opacity curve. An interesting feature of the expression (4.3-3) is that it is given in a separation-of-variables form, the variables being β_0 and y_0 that uniquely designate a point in the CRW. We believe that this approach can be adapted to other physical problems calling for opacity integrals in a ring-symmetric CRW .
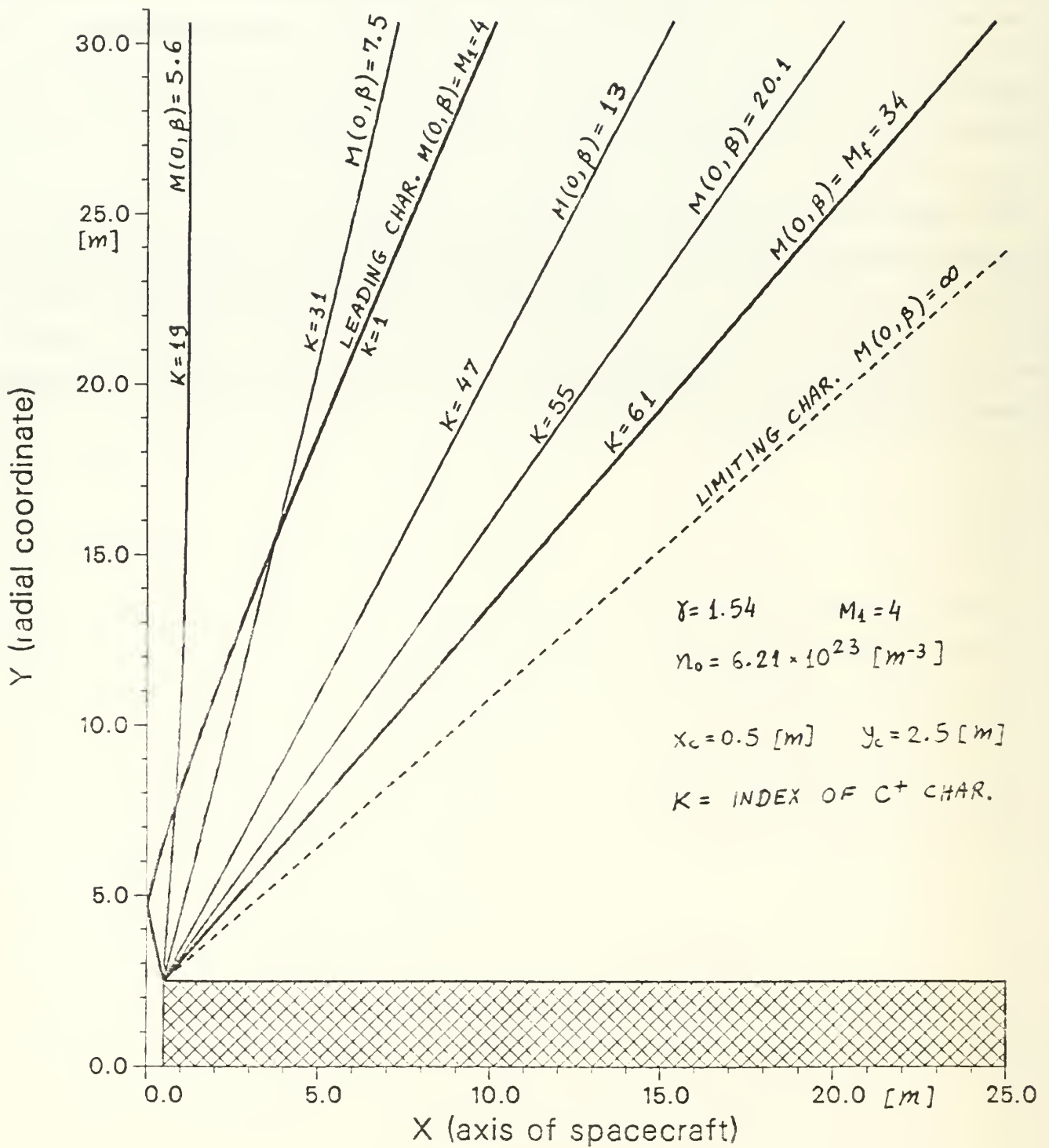
Figure 4-1.   Characteristics in Ring-Symmetric Jet

34

50.0

45.0

40.0 [m]

35.0

30.0

25.0

20.0

15.0

10.0

5.0

0.0

Y (radial coordinate)

$\beta=0.08$

$\beta=0.05$

$\beta=0.03$

$\beta=0.02$

LEADING CHAR. $M(0,\beta_1) = M_1 = 4$

$M(0,\beta) = M_f = 34$

LIMITING CHAR. $M(0,\beta) = \infty$

$\gamma = 1.54$ $M_1 = 4$

$n_0 = 6.21 \times 10^{23}$ $[m^{-3}]$

$D = 2.5 \times 10^{-10}$ $[m]$ $\sigma = \pi D^2$

$x_c = 0.5$ $[m]$ $y_c = 2.5$ $[m]$

BREAKDOWN SURFACES

$B = (U/\nu)\, \rho^{-1}\, (d\beta/dS) = \text{constant}$

0.0   5.0   10.0   15.0   20.0   25.0 $[m]$ 30.0

X (axis of spacecraft)
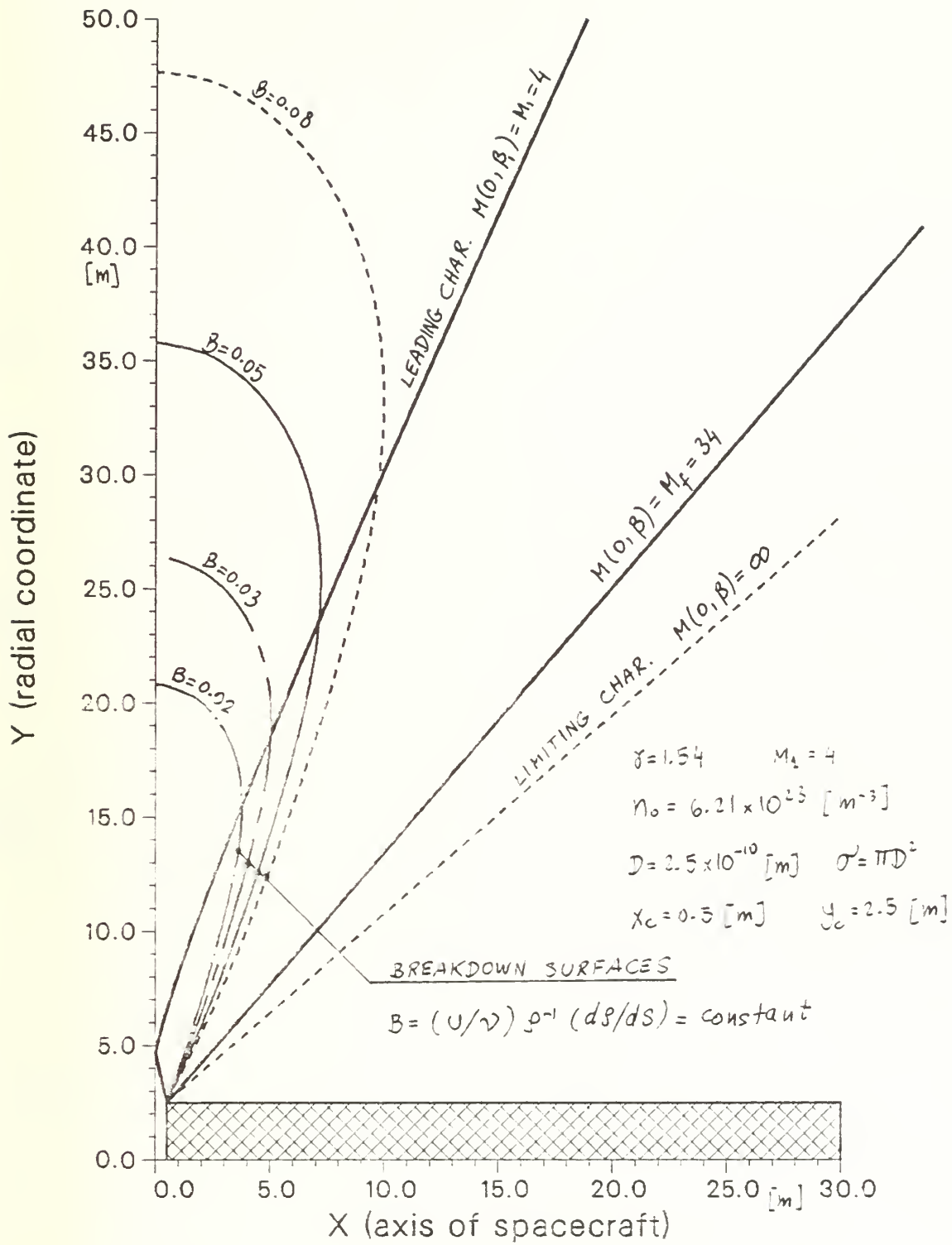
Figure 4-2.   Continuum Breakdown Surfaces in a Ring-Symmetric Jet

$$\tau(x) = \int_{x}^{x_L} \alpha \, n(x') \, dx'$$
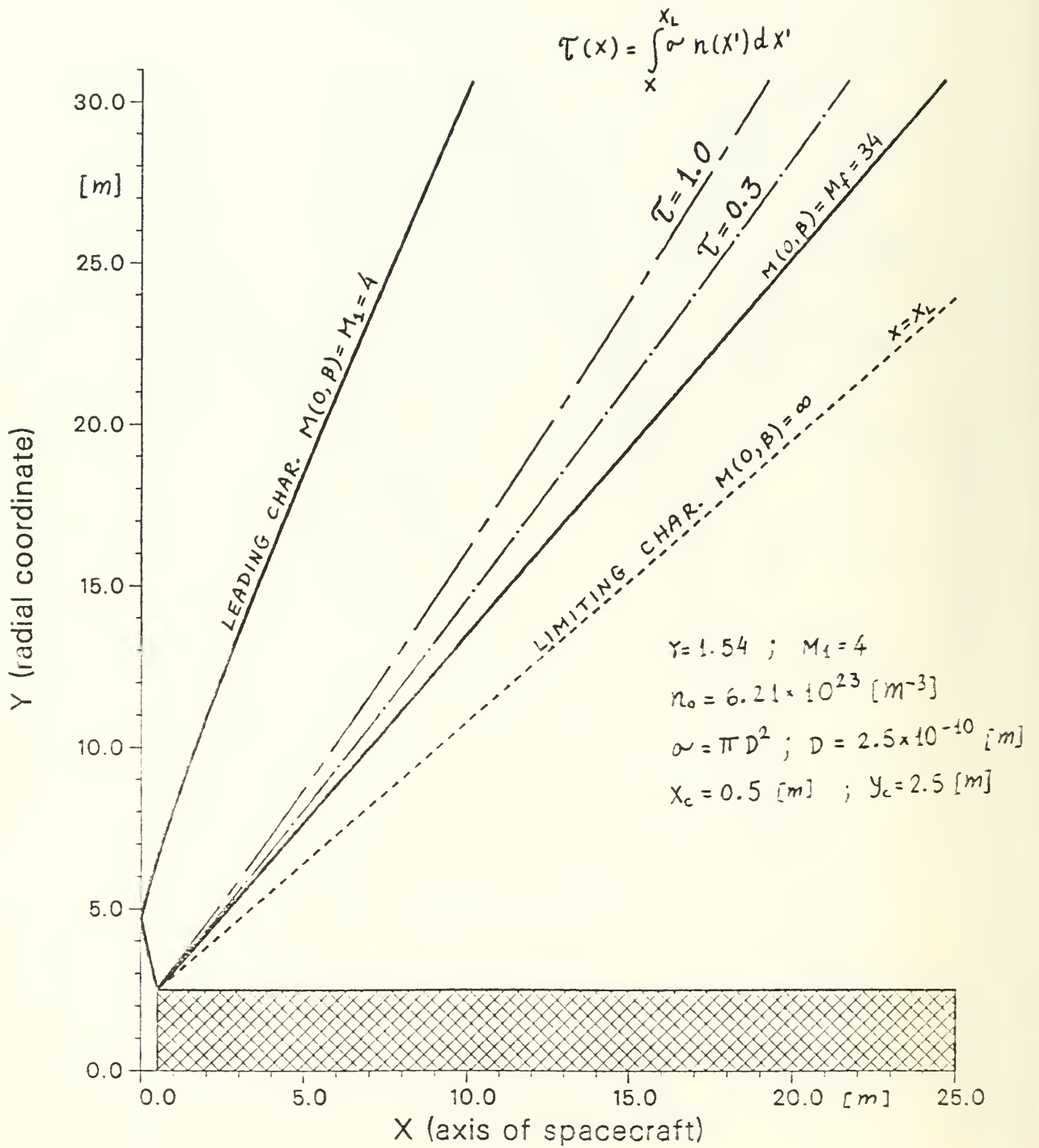
Figure 4-3. Constant Molecular Opacity (τ) Lines in a Ring-Symmetric Jet
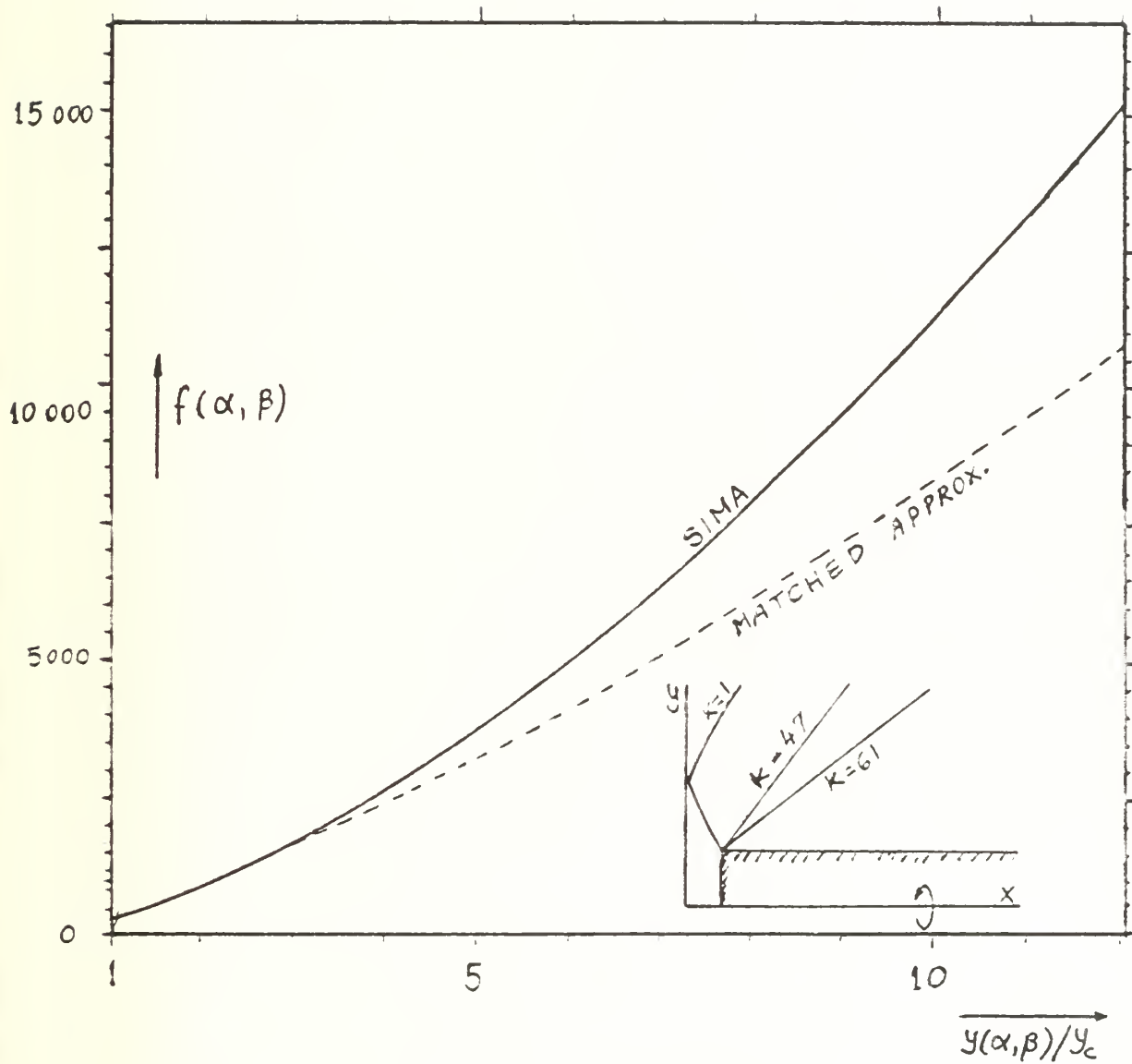
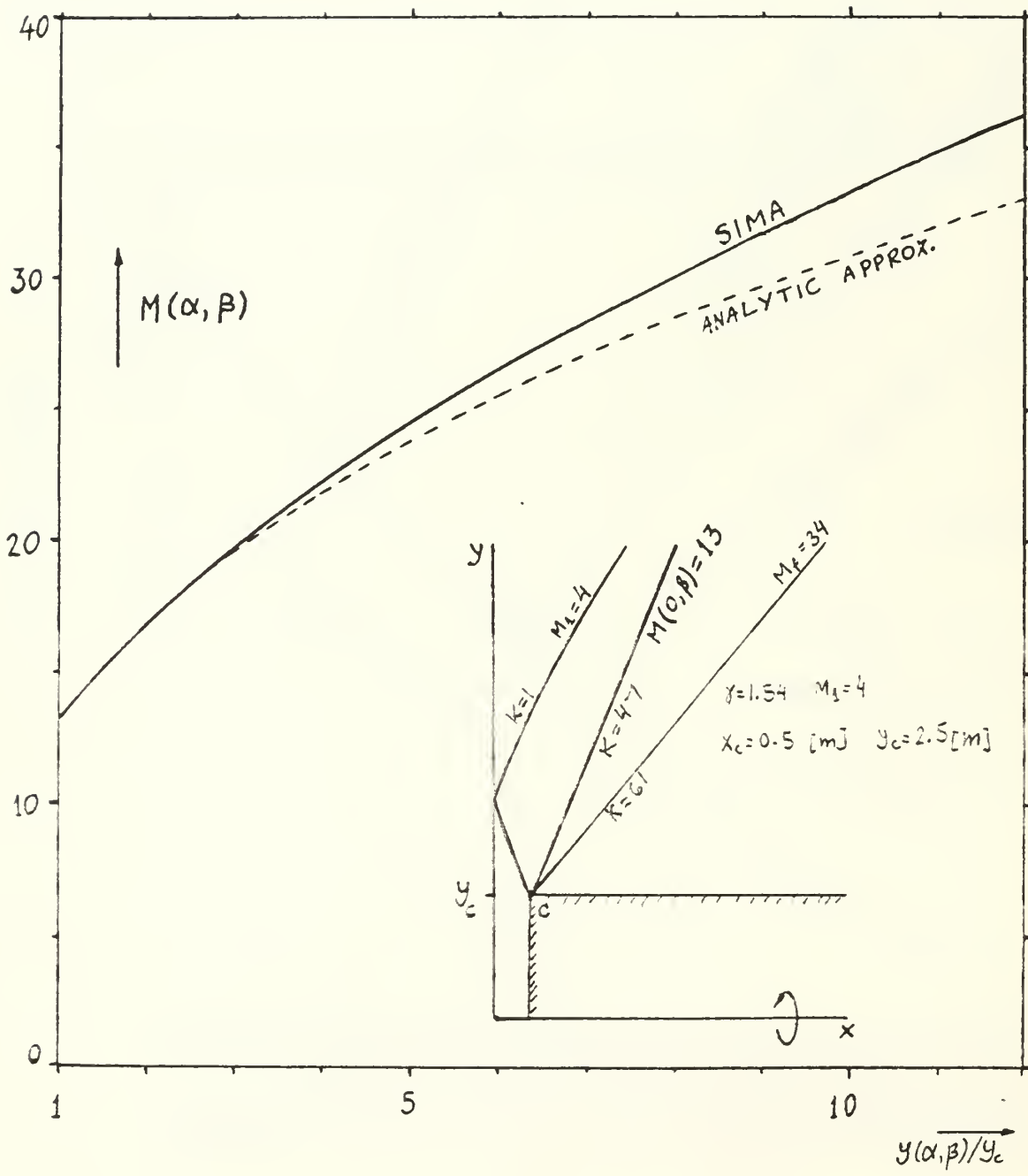Figure 4-4.   Variation of Area Ratio along Characteristic Line k = 47

37

Figure 4-5.   Variation of Mach Number along Characteristic Line k = 47
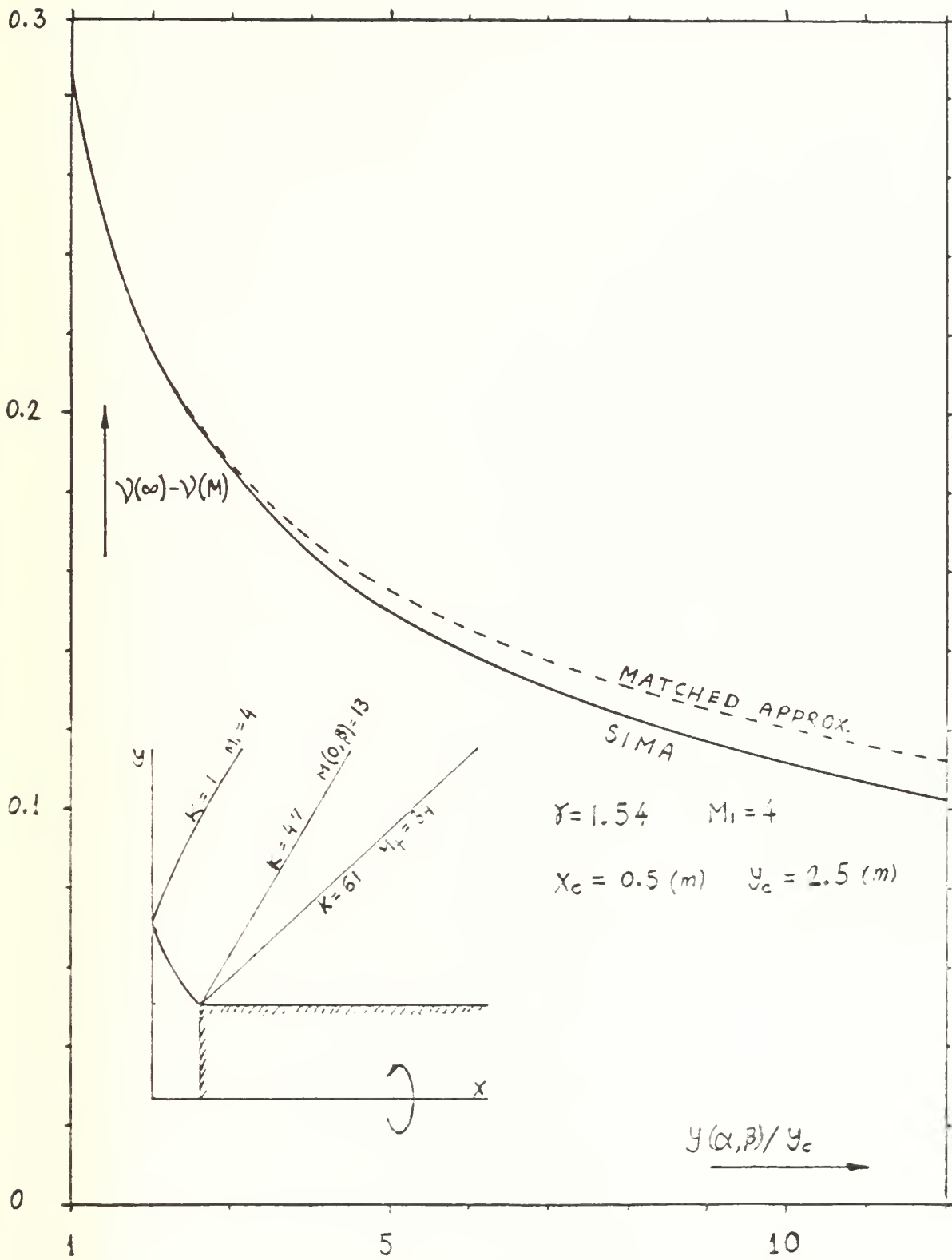
Figure 4-6.   Variation of Prandtl-Meyer Function along Characteristic Line k = 47

$$\tau(x) = \int_x^\infty \sigma \, n(x') \, dx'$$

ANALYTIC APPROX.

SIMA

PLANAR CRW (PRANDTL-MEYER)

y/y_c

$M_f = 3.4$

$y/y_c = 3.2$

$x - x_f$

$\gamma = 1.54 \quad M_i = 4$

$x_c = 0.5 \; [m] \quad y_c = 2.5 \; [m]$

$n_o = 6.21 \times 10^{23} \; [m^{-3}]$

$\sigma = \pi D^2 \quad D = 2.5 \times 10^{-10} \; [m]$

x

$\dfrac{x - x_f}{} \; (m)$

1.0

.5

0

4

3

2

1

0

-1.0

-.5

0

Figure 4-7.   Variation of Molecular Opacity τ along a Line Parallel to x axis

40

Figure 4-8.   Variation of Molecular Opacity τ along a Characteristic Line (k = 55)

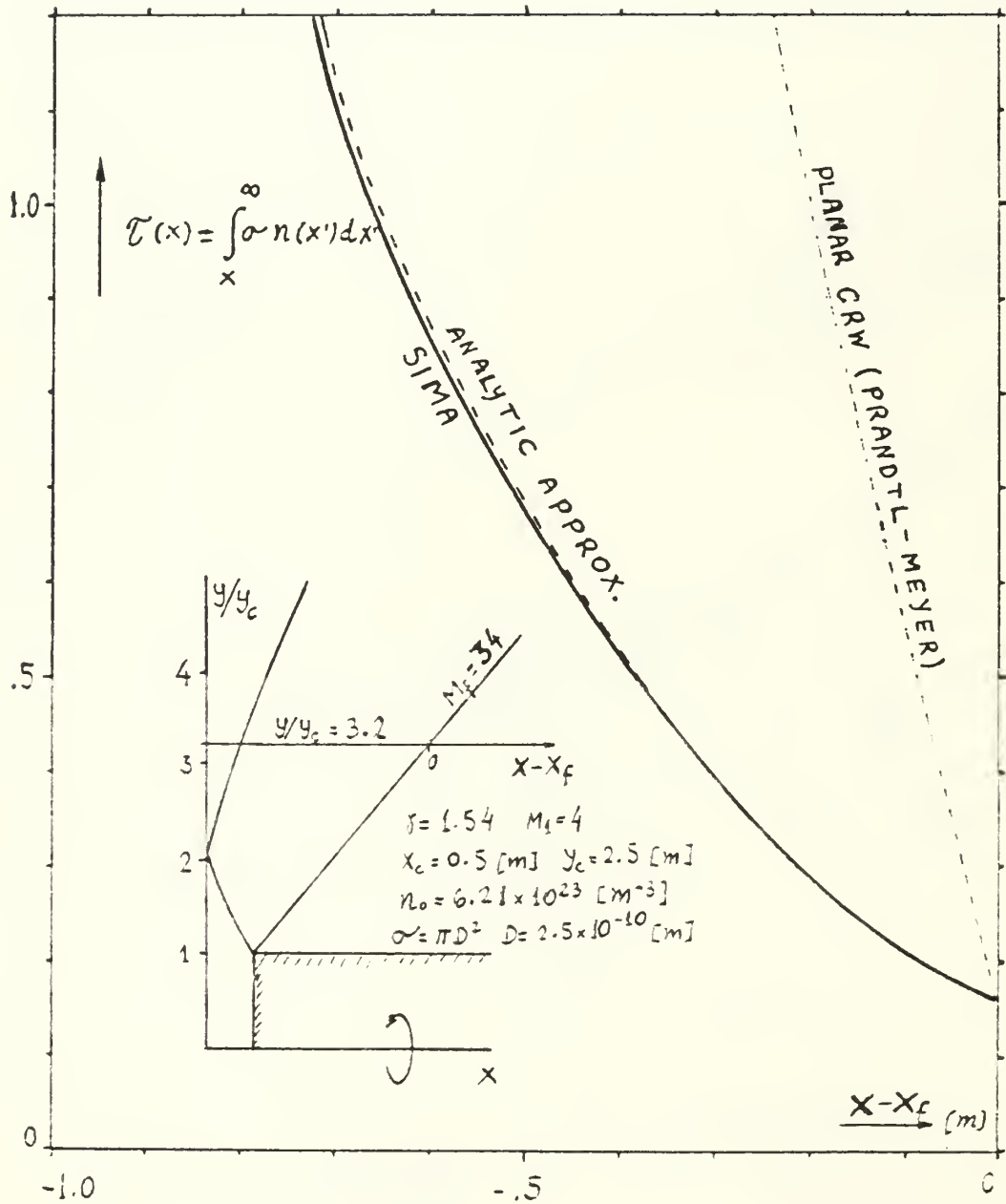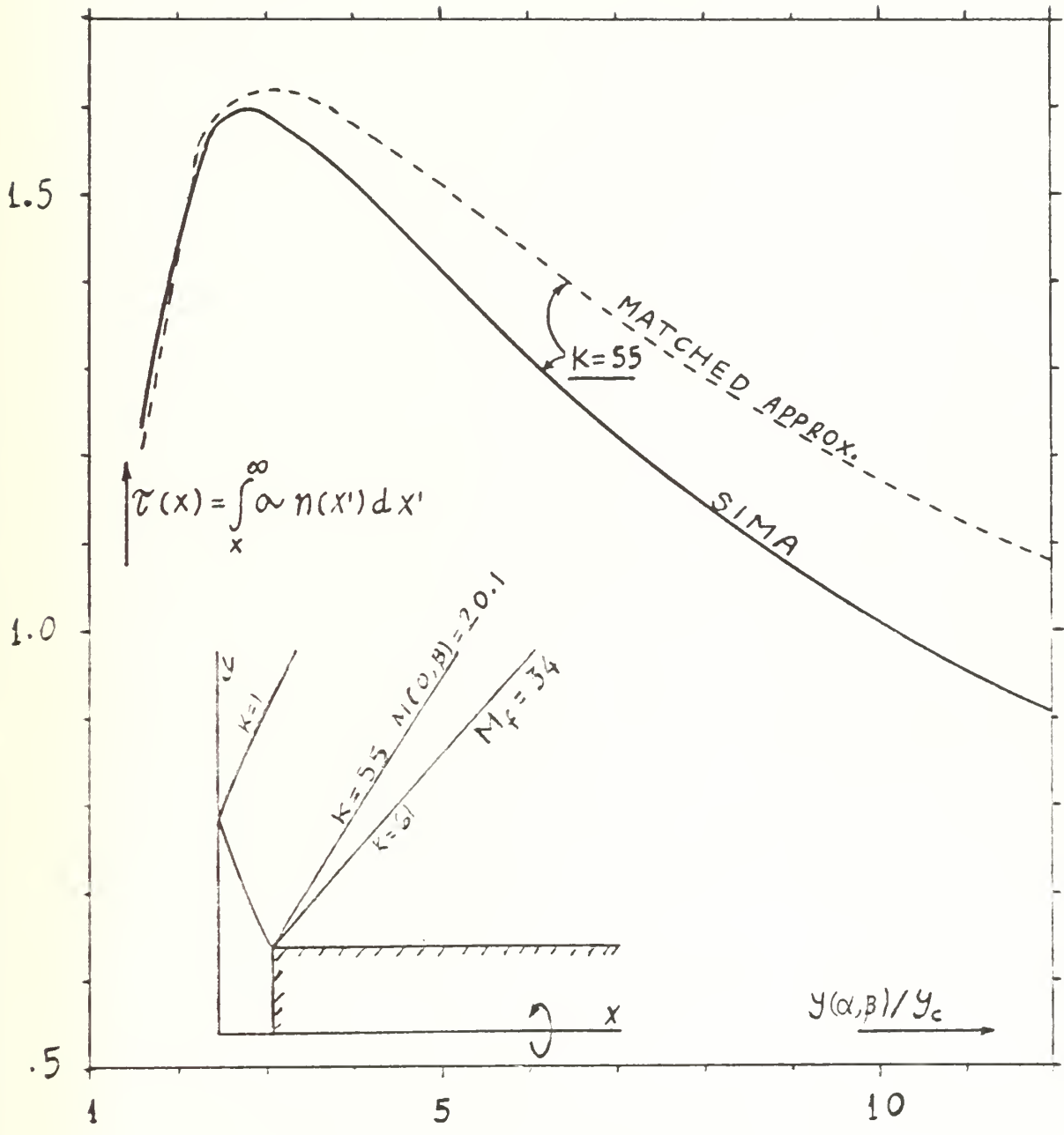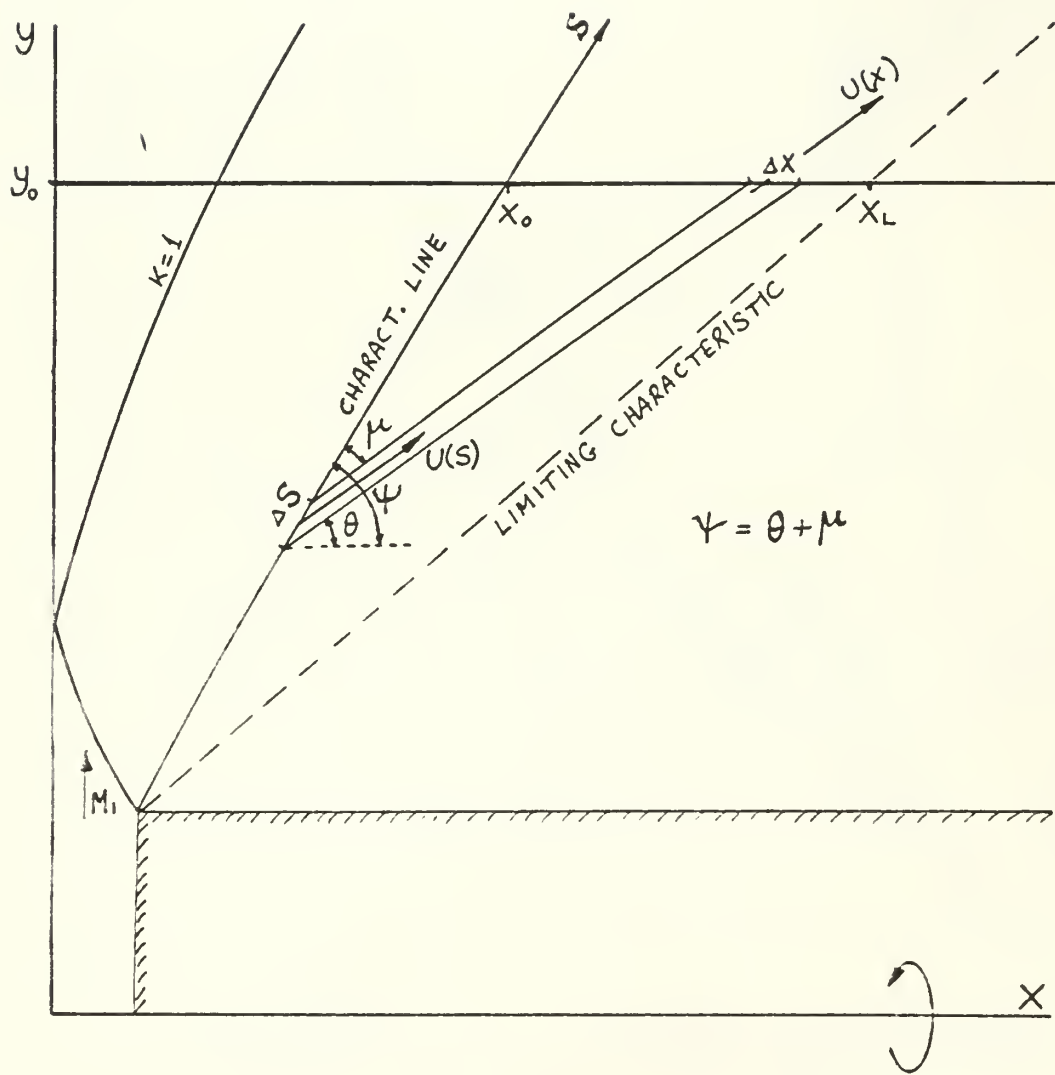Figure 4-9.   Schematic Description of Mass Conservation Law Enabling Transformation of Opacity Integral to Characteristic Line Passing through (x_0, y_0)

5. REFERENCES

[1] Falcovitz, J. and Fuhs, A. E., "Contaminating Sideflow from Supersonic Exhaust Jets in Space", 37th IAF Congress, Oct. 4-11,1986, Innsbruck, Austria. Paper IAF-86-29.

[2] Bird, G. A., *Molecular Gas Dynamics*, Clarendon Press, Oxford, 1976.

[3] Bird, G. A., "Breakdown of Continuum Flow in Free Jets and Rocket Plumes", Proceedings of 12th Symposium on Rarefied Gas Dynamics. In Volume 74, *Progress in Astronautics and Aeronautics*, Part II, p.681, Sam S. Fisher, Editor. Published by AIAA, 1981.

[4] Zucrow, M. J. and Hoffman, J. D., *Gas Dynamics*, John Wiley, New York, 1976.

[5] Ben-Artzi, M., and Falcovitz, J., "A High-Resolution Upwind Scheme for Qausi 1-D Flows", INRIA Workshop on *Numerical Methods for Solving the Euler Equations of Fluid Dynamics*. F. Angrand and R. Glowinski (editors). Paris, Dec. 1983. SIAM Publication, Philadelphia, 1985.

[6] Ben-Artzi, M., and Falcovitz, J., "An Upwind Second-Order Scheme for Compressible Duct Flows", *SIAM Journal on Scientific and Statistical Computing*, Vol 7, p.744-768, 1986.

[7] Ostwatitsch, K., *Grundlagen der Gasdynamik*, (in German), Springer-Verlag, Wien, New York, 1976.

[8] Liepmann, H. W. and Roshko, A., *Elements of Gasdynamics*, John Wiley, New York, 1957.

[9] Abramovich, S., "Gas Dynamics of Laser Exhaust External to Spacecraft", Naval Postgraduate School, Monterey, CA, Contractor Report NPS67-84-006CR, Nov. 1985.

[10] Falcovitz, J., "A Breakdown Surface Model for Thermal Backscattering from the Exhaust Plume of a Space-Based HF Laser", Naval Postgraduate School, Monterey, CA, Report NPS67-86-002CR, June 1986.

[11] Falcovitz, J., "Numerical Computation of Ring-Symmetric Spacecraft Exhaust Plumes", Naval Postgraduate School, Monterey, CA, Report NPS72-87-001CR, January 1987.

APPENDIX A.   PRANDTL - MEYER FLOW

Denoting by β the Mach number of the fan characteristic, the Prandtl-Meyer function [8] is given by :

$$v(\beta) = \Gamma^{1/2} \arctan\left[(\beta^2-1)^{1/2}/\Gamma^{1/2}\right] - \arctan\left[(\beta^2-1)^{1/2}\right]$$

$$\Gamma = (\gamma+1)/(\gamma-1)$$

(A-1)

In a C^+ wave, the Riemann invariant $(v+\theta)$ is uniformly constant. This leads (after some manipulation) to the following relations between the Mach number β and the C^+ characteristic angle ψ :

$$\psi(\beta) = \psi_L + \Gamma^{1/2} \arctan[\Gamma^{1/2} / (\beta^2-1)^{1/2}]$$

$$\beta^2 = 1 + \Gamma / \tan^2[(\psi-\psi_L)/\Gamma^{1/2}]$$

(A-2)

Where the characteristic angle and Mach angle are given by :

$$\psi(\beta) = \theta(\beta) + \mu(\beta)$$

$$\mu(\beta) = \arcsin(\beta) = \pi/2 - \arctan[(\beta^2-1)^{1/2}]$$

(A-3)

We now seek an expression for the distance η of a point on the transverse (C^-) characteristic from the corner. The following differential relation is derived from flow field geometry (Figure A-1) in a planar CRW :

$$\eta \, d\psi = - \tan(2\mu) \, d\eta$$

(A-4)

45

In order to replace $\Delta\psi$ by $\Delta\beta$, we use the following expression derived by differentiating the relation $\psi(\beta)$ given in Eq.(A-5) with respect to β :

$$\psi_\beta = - ((\gamma+1)/2)\,\beta\,(\beta^2-1)^{-1/2}\left[1+((\gamma-1)/2)\beta^2\right]^{-1} \tag{A-5}$$

Using (A-5), we eliminate $\Delta\psi$ from (A-4), getting :

$$(\ln\eta)_\beta = ((\gamma+1)/4)\,\beta\,(\beta^2-2)\,(\beta^2-1)^{-1}\left[1+((\gamma-1)/2)\beta^2\right]^{-1} \tag{A-6}$$

The right hand side of (A-6) is decomposed into two partial fractions, resulting in an integral consisting of the sum of two log functions. Thus, the dependence of η on β is the following product of two factors, normalized to yield $\eta(\beta_1)$ at the leading characteristic :

$$\eta(\beta) = \eta(\beta_1)\left\{\left[1+((\gamma-1)/2)\beta^2\right]/\left[1+((\gamma-1)/2)\beta_1^2\right]\right\}^{(\gamma/2(\gamma-1))}\left\{(\beta_1^2-1)/(\beta^2-1)\right\}^{1/4} \tag{A-7}$$

Since $\eta(\beta)$ is identical with the definition (3.1-2) of the characteristic variable α, by differentiating (A-7) with respect to α with $\beta = $ constant, we get Eq.(3.1-5) for η_α.

Now we turn to the other geometrical function needed in the analysis of the ring-symmetric CRW flow at the corner. The following geometrical relationship is established by inspection from Figure A-1 :

$$\Delta\xi = \Delta\eta / \cos(2\mu) \tag{A-8}$$

Where the ξ and η increments correspond to an increment in characteristic angle ψ, or to an implied increment in Mach number β. When $\Delta\eta$ is replaced by $\Delta\beta$ using (A-6) and when also $\cos(2\mu)$ is replaced by a β expression, we get a expression for ξ_β in terms of η and β. The α derivative of this last expression is Eq.(3.1-5) for $\xi_{\alpha\beta}$.
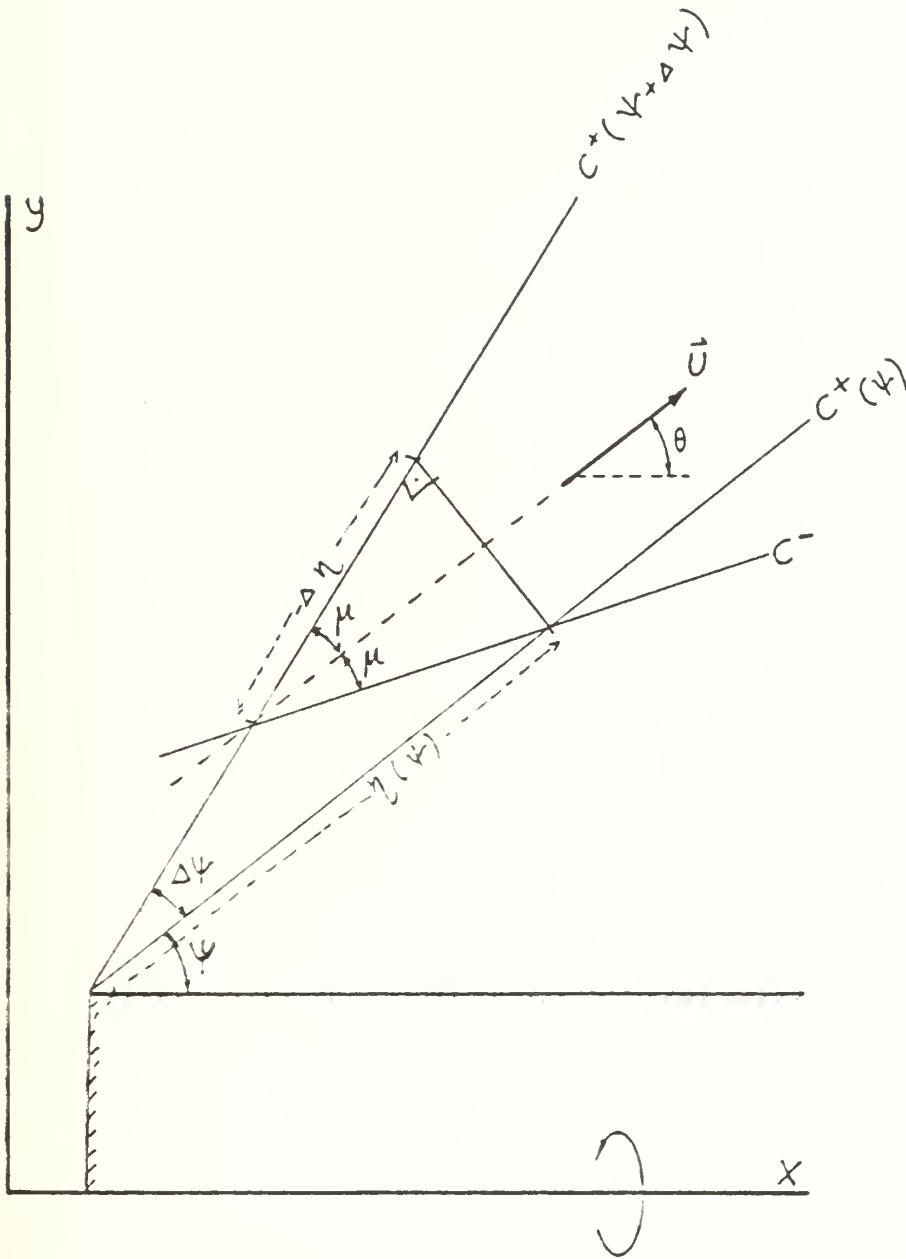
Figure A-1.   Geometry of Characteristics and Streamlines in a Prandtl-Meyer Flow

6. DISTRIBUTION LIST

1. Defense Technical Information Center
   Cameron Station
   Alexandria, VA 22314 2

2. Library, Code 0142
   Naval Postgraduate School
   Monterey, CA 93943-5100. 2

3. Department Chairman, Code 67
   Department of Aeronautics
   Naval Postgraduate School
   Monterey, CA 93943-5100. 1

4. Distinguished Professor Allen E. Fuhs
   Space Systems Academic Group, Code 72
   Naval Postgraduate School
   Monterey, CA 93943-5100. 5

5. Dr. Neil Griff
   SDIO/DEO
   Washington. DC 20301-7100. 3

6. Mr. Bruce Pierce
   SDIO DEO
   Washington. DC 20301-7100. 1

7. Dr. Joseph Falcovitz
   Code 72
   Naval Postgraduate School
   Monterey, CA 93943-5100. 10

8.   Professor Max F. Platzer
     Department of Aeronautics, Code 67
     Naval Postgraduate School
     Monterey, CA 93943-5100. 1

9.   Professor Oscar Biblarz
     Department of Aeronautics, Code 67
     Naval Postgraduate School
     Monterey, CA 93943-5100. 1

10. Professor David W. Netzer
     Department of Aeronautics, Code 67
     Naval Postgraduate School
     Monterey, CA 93943-5100. 1

11. Research Administration Office
     Code 012
     Naval Postgraduate School
     Monterey, CA 93943-5100. 1

12. Dr. P. Avizonis
     Air Force Weapons Laboratory
     Kirtland Air Force Base. NM 87117 1

13. Dr. John Lawless
     Space Power Inc.
     1977 Concourse Drive
     San Jose. CA 95131 1

14. Dr. Mark Thornton
     Boeing Aerospace Company
     Post Office Box 3999
     Seattle, WA 98124-2499 1

15. LT. Mark Price
    AFRPL
    Edwards AFB, CA 93523 1

16. Mr. Arthur W. Rogers
    Space Systems Division
    Hughes Aircraft Co.
    P. O. Box 92919, Los Angeles, CA 90009 1

17. LCOL Rick Babcock, USAF
    Air Force Geophysical Laboratory
    Hanscomb Field
    Bedford, MA 01730 1

18. Dr. James Stark Draper
    Aerodyne Research, Inc.
    45 Manning Road
    Billerica, MA 01821 1